This document was prepared in conjunction with work accomplished under Contract No. DE-AC09-76SR00001 with the U.S. Department of Energy.

DISCLAIMER

TECHNICAL DIVISION
SAVANNAH RIVER LABORATORY

DPST-83-722

August 2, 1983

M E M O R A N D U M

TO: R. L. FOLGER

FROM: D. H. TAYLOR

REPORT OF IRIDIUM/$^{238}PuO_2$ COMPATIBILITY TEST

INTRODUCTION AND SUMMARY

The Savannah River Plant (SRP) makes $^{238}PuO_2$ general purpose heat sources (GPHS) to power radioisotopic thermoelectric generators (RTG) for NASA deep space probes. After being fabricated into ceramic pellets approximately one-inch-long by one-inch in diameter, the PuO_2 is encapsulated in a 0.028-inch thick iridium shell which is vented on one end to permit escape of the decay helium. The major purpose of the iridium shell, or clad vent set (CVS), is to provide containment of the plutonium dioxide in the event of a mission failure involving a high velocity impact of the GPHS capsules with the ground. Safety verification impact tests (SVTs) of the capsules are performed at Los Alamos National Laboratory (LANL). In September 1979 a safety verification test of a fuel form of an earlier, spherical, design showed catastrophic failure of the iridium containment shell. Investigation of this failure by an interagency task force suggested that the failure was caused in part by small amounts of phosphorus on the grain boundaries of the iridium shell. Further study showed the PuO_2 fuel to be the primary source of phosphorus. The present study was undertaken in response to the findings of the task force. The work was performed jointly by personnel from Savannah River Laboratory (SRL), LANL, and Oak Ridge National Laboratory (ORNL) and had the following objectives.

- Assess the compatibility of the present chemical purity of the PuO_2 and the iridium alloy currently used to fabricate clad vent sets.
- Establish limits for phosphorus (P) concentration in the PuO_2 fuel so as to minimize phosphorus transport to the iridium cladding.

- Assess the effects of other major impurities in the fuel such as calcium (Ca), aluminum (Al), silicon (Si), and iron (Fe) on phosphorus transport.
- Assess the effects of these impurities on vent plugging and metallurgical properties of the iridium cladding.
- Assess the effectiveness of vacuum outgassing of the fuel in preventing vent plugging

The overall results of this study indicate that the chemical purity of the fuel used presently to fabricate fueled clad vent sets will not present any special problems to the performance of the fueled clad vent sets as intended. However cation impurities in the fuel can have a deleterious effect on the iridium cladding and vents and should be minimized as much as practical. Fueled capsules for which the PuO_2 has a Ca, Al, or Si content greater than about 100 ppm might present some problems. These capsules might have large quantities of deposits in the vents if they are stored at elevated temperatures for several months.

Other findings from the study were:

- The P concentration in the PuO_2 fuel should not exceed approximately 15 ppm to minimize transport of P into the Ir cladding. The effects of other major impurities on phosphorus transport could not be determined because the test did not compare fueled capsules having equivalent levels of P but different levels of the other impurities.
- The effects of the major impurities are to enhance Pu vaporization out of the CVS, enhance grain growth in the Ir cladding, and contribute significantly to plugging of the vents.
- Vacuum outgassing as a final step may contribute to vent plugging.

Precise limits or specifications on impurities cannot be set based on the limited four capsule experiment. Any reduction of the impurity level will, however, improve the Ir/PuO_2 compatibility.

EXPERIMENTAL PROCEDURE

Four full-scale GPHS pellets (serial numbers 44, 45, 48, and 49) were made by SRL in the Plutonium Experimental Facility (PEF) using Technical Standard centerline fabrication conditions and standard $^{238}PuO_2$ feed powder. The test matrix is given in Table 1. Pellet 44 was made using standard conditions, including vacuum outgassing of the heat treated pellet and background (undoped) concentrations of phosphorus and other cationic impurities. Pellet 45, was identical to 44 but was not vacuum outgassed. (Feed for Pellet 45 was not from the same batch but was still standard feed.) Pellet 48 was considered a standard pellet, but was doped

with 20 to 30 ppm phosphorus. Pellet 49 was doped with P, Ca, Al, Si, and Fe and fabricated in the standard way. The impurities were added by first slurrying the PuO_2 with a solution of H_3PO_4 and Na_2SiO_3 and evaporating to dryness. The powder was then slurried again in a solution of $Al(NO_3)_3$ and $Ca(NO_3)_2$ and evaporated to dryness. Fe was added as $Fe(NO_3)_3$. However, spark source mass spectroscopy (SSMS) showed that for all of the pellets in this test, the background concentration of Fe was so high that those pellets which had been doped with Fe could not be distinguished from those which had not. The source of this background Fe is not known.

A slice was cut from each heat treated or vacuum outgassed pellet prior to encapsulation for use as control specimens. Pre-aged metallography and chemical analysis was performend on these specimens. The remainder of each pellet was encapsulated by SRP in the Plutonium Fuel Form (PuFF) Facility using near flight quality type iridium cups and forwarded to LANL. At LANL the clad pellets were enclosed in two-pellet GPHS graphite impact shells (GIS's) made of FWPF-3D carbon-carbon-composite and prebaked to duplicate the condition of the flight hardware in order to simulate expected service conditions (temperature gradients, etc.). The samples were aged at LANL at RTG operating temperatures (Table 2). No re-entry thermal pulse was given the samples. After aging, the capsules were sectioned for chemical analysis and metallurgical characterization.

The iridium cups used in the test were chosen to be as close to flight quality as possible. Cups used for Pellets 44 and 45 had numerous dye penetrant indications plus a grit blasted surface below the minimum requirement. Cups used for Pellets 48 and 49 had a wall thickness over maximum. Archive rings from each cup were used for control samples. Each ring was cut in half. One half was used to characterize the bulk and grain boundary chemistry and grain size in unaged iridium. The other half was used to characterize the iridium after aging at temperature but not in the presence of PuO_2. Prior to any analyses, the archive rings were given a one-hour heat treatment at 1500°C in vacuum to provide them with the same thermal history as the iridium cups.

As an additional control, two unvented cups were welded together empty. The empty welded clad (designated T-40) was heated unfueled in a GIS. Because this clad had no vent, impurities could only be introduced into the iridium by diffusing in from the outside.

The orientation of the capsules during aging was indexed so that capsules could be sectioned in a manner that would allow observed features to be related to the aging position. The configuration of the capsules in their graphite fixtures during aging is shown in Figure 1.

The test conditions are given in Table 2.

SUMMARY OF Ir/PuO_2 COMPATIBILITY TEST RESULTS

EFFECT OF AGING ON PuO_2 FUEL

PuO_2 Chemistry (Tables 3 through 5)

- The impurities of most concern are Si, Ca, Al, P, Mg (magnesium), Fe, Cr (chromium), Ti (titanium) (see Table 4 for current specifications).

- Both SSMS and electron microprobe analysis (MP) showed the above impurities to be inhomogeneously distributed in the PuO_2. This inhomogenity is both local (on grain boundaries rather than in solid solution for Ca, Si, Al) and regional (some regions of the pellets have higher concentrations than others). MP showed that iron and phosphorus were more homogeneously distributed on a local level. With the exception of Fe and Cr, changes in the bulk concentrations of the impurities during aging were less than the sensitivities of the analytical techniques used to measure them. Fe and Cr were reduced by up to two orders of magnitude during aging.

- Large quantities of Al, Ca, and Si added to Pellet 49 formed a second phase in the grain boundaries during fabrication. During aging these elements were redistributed to the pores and free surfaces such as internal cracks (Figure 2). Transport out of the fuel, most likely by vaporization, followed a pathway of migration from the interior of the fuel to free surfaces (e.g. cracks). A small amount of second phase deposit was also seen in Pellet HF-2 (from ECT-1). Impurities in Pellet HF-2 were Si, 170 ppm; Al, 268 ppm; Ca, 75 ppm. Current specifications for each of these impurities are Si, 200 ppm; Al, 150 ppm; and Ca, 100 ppm. The presence of an identifiable second phase in Pellets HF-2 and 49 suggests that the specification limits for Si, Al, and Ca ought to be set lower than about 100 ppm since no second phase has been observed in pellets for which these three impurities were less than about 100 ppm (which is normally the case for production pellets).

- Impurities present in the pre-aged fuel at different levels were not reduced during aging to a common or "equilibrium" value.

- Although the composition of Pellet 48 was intended to differ from Pellets 44 and 45 only in P, evidence from examination of the vents and cladding suggests that the composition of Pellet 48 was significantly higher in elements such as Si. Bulk analyses by SSMS and emission spectroscopy (ES) were conflicting and could not resolve this issue.

Fuel Structure

- Generally, aging tended to slightly densify the fuel. Grain size increased by up to a factor of approximately two.
- Aging does not significantly multiply the number of cracks in the fuel.

EFFECT OF AGING ON IRIDIUM CLADDING

Iridium Microstructure

- The grain size of the fueled cups is greater in all cases than that of the aged archive rings or unfueled aged cups (Table 6, (Figures 3 through 7).
- The interior grains of the fueled iridium cups (those nearest the fuel) are larger on average than the grains at the center of the thickness of the cups or at the exterior of the cups (Table 6).
- The interior and exterior grains of the unfueled aged cups are also slightly larger than the center grains of their cups (Table 6).
- The grain size of the aged archive rings is essentially uniform across the thickness (Table 6, Figures 3 through 7).
- The vent cup of Pellet 48 (P-701-4) had areas of widely varying grain size with very large grains on both interior and exterior surfaces. The shield cup on Pellet 49 (PR-715-2) also showed areas of variable grain size (variable refers to fluctuations in grain size in the direction parallel to the longtudinal axis of the cups and at the same depth) with areas of unusually large grains on the exterior surface (Table 6, Figure 5).
- The effect on iridium microstructure of the different pellets was only evident as a larger average grain size for the vent cups of Pellets 48 and 49 (Table 7).

Iridium Chemistry

- Phosphorus (P) was detected by Auger electron spectroscopy (AES) in the cladding of Pellets 48 and 49 corresponding to the levels in the fuel. The AES analysis for this and all samples was taken using an electron beam with a 15 μm beam diameter. Spectra were obtained from three locations on each Ir sample: about 100 μm from both the inside and outside edges and one in the center of

the cross section. For CVS 48 with 20 ppm P in the fuel, P was not detected uniformly on the Ir grain boundaries. Instead it appeared in patches and was found only at the center and exterior surface of the cups. With CVS 49 which had 35 ppm P in the fuel, P was detected throughout the Ir grain boundaries. In contrast, P was not detected in the iridium cladding of Pellets 44 and 45. P in both of these pellets was less than 10 ppm. Based on this result we are recommending a maximum P level in the fuel of less than or equal to 15 ppm. The effect on P transport by other impurities could not be determined in this study.

- For Capsules 48 and 49, P was detected at Ir grain boundaries by AES, but its presence could not be correlated with grain growth. For example, the shield cup of Capsule 48 (N-502-3) had uniform Th content and grain size across the thickness at the location examined by AES (different from that shown in Figure 5). P was detected at grain boundaries of center and exterior grains and not on the interior grain boundaries. No large grains associated with the location of the P were observed.

- Th was investigated by SSMS, AES, and secondary ion mass spectrometry (SIMS). No significant change in bulk concentration was found by SSMS (Table 8). AES results suggested a general Th depletion on the grain boundaries of all fueled aged cups compared to aged archive rings (Table 9). The interior grains showed the most depletion, the center grains the least and the exterior grains depletion intermediate between that of the center and interior grains (Table 9). A plot of Th content for each region (exterior, center, interior) averaged over all cups versus grain size for each region averaged over all cups showed a fairly linear correlation, with the grain size increasing as the Th content decreased (Table 10, Figure 8). Comparing the CVS for each capsule, the average Th content of each CVS did not significantly differ one from another (Table 7). However, with respect to individual cups, the Th content of the vent cup of Capsule 48 is greater than one standard deviation lower than the average Th content of all cups and the Th content of the shield cup of Capsule 49 is greater than one standard deviation higher than the average of all cups. Hence, the effect of impurities on the Th content of the iridium cladding is inconclusive. The SIMS data showed Th on the grain boundaries. The number of Th inclusions appeared to be fewer than for unaged iridium.

- The Ir was analysed for several other elements using SIMS, SSMS, and ES. The SSMS samples were run with standards and were accurate to within about $\pm$30%. The results for key elements follow (also see Table 8).

- Tungsten (W). No change in W concentration was reported by SIMS. The results of the SSMS analyses were unclear. In all cases but one (Pellet 45), the W level was reported to have increased by a factor of 2 to 3. Since the precision of the measurements is about ±30%, the measured increase is apparently real. However, since there is no known source of W at present the measured increase in W is not understood. W is added to the Ir to increase the recrystallization temperature and thereby inhibit grain growth. Normally W is homogeneously distributed throughout the Ir.

- Silicon (Si) was found along the grain boundaries in the Ir by SIMS at only low levels. No metallographic evidence for any second phase was found except near the vent holes. Hence, fracture along the longitudinal side of the CVS's due to a brittle Ir/Si intermetallic is unlikely. SSMS showed a slight increase in bulk Si content from less than or equal to 1 ppm to approximately 7 ppm. The weld in Sample 45 was measured at 20 ppm. Samples of weld areas were not available for examination by SIMS for Si along grain boundaries.

- Iron (Fe) and Chromium (Cr) were detected in large amount by SIMS in the Ir. Nickel (Ni) was also detected, but in smaller quantities. For Capsule 49 the concentration was maximum at the interior surface (approximately 1/2 atom % for Fe) and decreased to background at a depth of about 150 μm. For Capsule 44, the maximum concentration of Fe and Cr was approximately the same as that of Capsule 49 at the surface but the depth of penetration was only about 30 μm. The concentration of Fe and Cr at the surface of Capsule 45 was also approximately the same as for Capsule 49. The depth of penetration was about midway between Capsules 44 and 49. SIMS showed that the concentration of Fe and Cr was maximum at the iridium grain boundaries and fell off with depth into the grains from the grain boundaries. Near the surface of the iridium the concentration fell off very little from the maximum at the grain boundary. However, the fall off became sharper with depth into the iridium until at the maximum depth of penetration, the Fe and Cr were located only at the grain boundaries. Fe was also shown to diffuse more rapidly along the grain boundaries and into the bulk iridium. The SIMS data graphically demonstrate that the Fe and Cr diffuse rapidly into the Ir along grain boundaries and from the grain boundaries into the bulk iridium. Fe and Cr were not detected at the grain boundaries by AES. However, the AES spectra were taken at about 100 μm in from the edge of the iridium where the Fe and Cr concentration had fallen off sharply and was probably below the detection limits of the

Auger spectrometer. Previous work at ORNL[1] could detect no effect of Fe on grain size for concentrations of Fe in the Ir up to 300 ppm. Higher concentrations were not evaluated, but no effects on grain size of Fe and Cr could be positively identified in the present study. The boundary of the Fe and Cr diffusion layer was not as deep as the boundary of the large grain size. In addition the Fe and Cr diffusion boundaries for Ir clads of Capsules 44 and 45 were at different depths whereas the boundaries of the large grains were about the same as for Capsule 49. Hence, Fe and Cr probably do not have a strong effect on grain growth.

- Calcium (Ca) was not observed at the grain boundaries by SIMS. No change in the Ca level was observed by SSMS for any sample except Capsule 49. There the Ca increased six-fold from 0.5 ppm to 3.0 ppm.

- Aluminum (Al) was found by SIMS to correlate with the presence of Fe and Cr, decreasing as the inverse of the increase in the Fe and Cr concentration. In particular the concentration of Al at grain boundaries was specifically lowered where Fe and Cr were present. The bulk concentration measured by SSMS was erratic. Some samples showed an increase by nearly a factor of two, while others showed no increase. At concentrations up to about 100 ppm ORNL[1] found that Al appeared to improve impact ductility. From the SIMS and SSMS results of the present work the effect on impact ductility of the changes in Al concentration and distribution appear indeterminate. If the effect of the Al results from its presence on grain boundaries, then the ductility is probably impaired by the Fe and Cr. If the effect of the Al depends on its bulk concentration, then the Fe and Cr probably have relatively little effect since the bulk Al concentration did not seem affected except near the inner edge.

EFFECT OF AGING ON VENTS

Vent Chemistry

- In general, impurities volatilizing from the fuel deposit on interior surfaces of capsules as well as in vents. The extent of this deposition varies from sample to sample and with location within the sample.

- No deposits around the vent holes on the exterior of the clads were observed for Capsule 45 (not outgassed, Figure 9). Minor surface deposits were found on Capsule 44 (Figure 10). Very extensive deposits of impurities (approximately 6.3 mg) were found forming a cone around the vent of Capsule 49 (Figure 11).

Deposits around Capsule 48 vent hole (Figure 12) were heavier than for Capsule 44, but these may have come from Capsule 49 by vapor migration through the holes in the graphite floating membrane separationg Capsule 48 from Capsule 49. Evidence for this can be seen by the hexagonal pattern of spots visible on the Ir of Capsule 48 which correspond to the holes in the graphite membrane.

- Capsule 45 had the least deposits in the filter elements. Capsules 44, 48, and 49 all had large amounts of material deposited in the filter elements (Figure 13). Considering all the photomicrographs of the filter elements (not just those shown in Figure 13) Capsule 49 was judged to have more material in the filter elements than Capsules 44 and 48.

- Deposits of about the same composition as those observed in the vent filter elements were also observed around the vent holes.

- Microprobe analysis of the deposits in the vents (filter element and vent hole) showed these deposits consisted of a major phase and one or more minor phases. The major phase consisted of the dopant elements (Ca, Al, Si, P, and Pu) in various amounts as well as some unexpected elements present in the fuel at low levels (e.g. Mg, Ti).

- The major phase was found throughout the filter elements.

- The qualitative composition of the phases found in each capsule vent are given in Table 11.

- For undoped fuel samples, the major impurity phase in the filter elements consisted of Ca, Si, Mg, and Pu (similar to that for Capsule 48, Figure 14, except richer in Si and Mg, and having no P).

- The material in the vents of Capsule 48 reflect the P in the fuel. Microprobe data suggest the phase formed in the undoped sample vents was modified in Capsule 48 by P replacing Si (Figure 14). This substitution is common for compounds with phosphates and silicates.

- The effect of the high concentrations of Si and Al are apparent in the major phase in the vent of Capsule 49. Even though P is present, the extra Si in the fuel evidently led to an increase in Si in the deposit (Figure 15). The excess Al replaced the Mg. This phase was decorated with dendrites of Ca-Pu which appear to have recrystallized from the compound suggesting the compound may have been liquid at the aging temperature.

- Near the center of the vents, deposits of nearly pure SiO_2 are found reflecting the high volatility of the Si-O species.

- At the surface near the vent hole intermetallic compounds of Ir, Si, and Pu begin to form (Figure 16).

- In Capsule 48 an Ir-W intermetallic is observed in the vent hole (Figure 17).

- In Capsule 49 Ir-Ti and Ir-Al intermetallics begin to form.

- Deposits of Ca, Al, and Si are found in the grain boundaries near the vent hole in Capsule 49 (Figure 18).

- The numerous minor phases show the complexity of the volatile species. It is significant that they contain no other elements than those contained in the major phases.

- The results show that the additions of large amounts of Ca, Al, and Si increase the volatilization of Pu. Pu analysis of the graphite surrounding Capsules 48 and 49 show the Pu transport out of the capsules to be approximately ten times greater than for undoped Pellets 44 and 45 (445 μg vs. 61 μg). However, the recovery of the effusate surrounding the vent hole of Capsule 49 (6.3 mg) shows the amount of Pu volatilized is probably several orders of magnitude greater than for undoped samples.

EFFECT OF VACUUM OUTGASSING

The vent in Capsule 45 was noticeably more free of deposits than the vents of the other three capsules. It is unlikely that this result is due to a significantly lower level of impurities in Pellet 45. For example, chemical analyses of Pellets 44 and 45 by both SSMS and ES found no significant difference in their composition. Moreover, even where the composition was significantly different, as for Pellets 44 and 49, the resulting deposits in the vents were more similar than between Capsules 44 and 45. It is possible that the significantly reduced material transport observed in Capsule 45 was due to a higher oxygen activity of Pellet 45 resulting from lack of vacuum outgassing. Work reported by Battelle Columbus Laboratories in 1973[2] on mass transport within encapsulated MHW fuel points out that increased oxygen activity not only increases vaporization of Ir as IrO_3, it is expected to decrease the vaporization of volatile impurities such as Ca, Si, Fe, Cr, and Ni (Al was not mentioned specifically in the Battelle report, but should behave in an analogous way to the other cations). The decrease in volatility with increasing oxygen pressure should be generally true for these cations whether they are present as binary, ternary, or higher compounds as long as they are present as oxides.

Recent work at SRL[3] on the effect of atmosphere on impurity retention showed that heating PuO_2 doped with Ca, Al, Si, and P in vacuum at 1500°C removed more than twice as much by weight of the impurities than heating in flowing oxygen for the same length of time at the same temperature. Since the oxygen was flowing, the vapor species above the samples would be effectively removed in both cases. Hence, the different loss rates would be due more to differences in oxygen activity rather than evaporation kinetics. Si was found to volatilize more readily than either Ca or Al.

In the present study, Ir transport was only noticeable in the vent of Capsule 48 which had been outgassed. However, deposits of vaporized elements were present in all capsules, suggesting that vaporization of impurities from the fuel is more important to control than vaporization of Ir from the cladding. The analysis of the effusate on Capsule 49 suggests the same. The effusate had large amounts of Ir and W (Table 3). However, the major constituent was PuO_2. Large amounts of Ca, Al, and Th were also present. Hence, even though vaporization of Ir occurred, vaporization of the fuel and its impurities was much greater (the fuel had >600 ppm Th).

From the results of this study as well as the results of the other two studies cited it appears that a final vacuum outgassing step may aggravate vent plugging. The evidence of these studies suggests that a better regimen for post hot pressing heat treatment would be to give pellets a 6 hour vacuum outgassing immediately after hot pressing and follow this with a low temperature (700°C) final heat treatment in oxygen. The high temperature vacuum outgassing would reduce impurity levels and enlarge grain size with minimum crack growth; the low tmperature oxygen heat treatment would burn off carbon from the die and restore stoichiometry to enhance the oxygen activity in the CVS. Preliminary work by SRL and SRP has shown that low temperature reoxidation does not lead to the same degree of pellet cracking as high temperature reoxidation. This change could only be implemented in future programs after additional study and impact testing.

The above interpretation for the differences in vent plugging is not unanimously shared by members of the heat source community. It has been pointed out, for example, that some of the MHW fuel sphere assemblies had plugged vents after aging, but had not been vacuum outgassed prior to aging. The author agrees that the statistics of the present study are too limited to permit demonstration of any mechanism. However, I am inclined to weight the evidence from this study heavier than the evidence from other work because this study was designed to compare the results of each encapsulated pellet against the others: the fabrication histories and chemistry of all of the components have been investigated and the aging conditions were as similar as possible. Hence it is more valid to make comparisons among the present fueled capsules than among the present capsules and other clad fuel for which their fabrication histories are not well understood. The apparent conflicts point to a need to do repeat controlled compatibility studies to provide enough statistics to establish a mechanism.

CONCLUSIONS

Vent plugging has been a major concern of the heat source program, although, with one exception, none of the vents have plugged tightly enough to cause swelling of the iridium capsule. Multi-hundred watt (MHW) test fuel sphere assemblies were found to emit decay helium in bursts rather than continuously which suggests intermittant plugging. The one GPHS capsule vent test performed (ECT-1), also showed intermittent plugging in which the vent plugged, reopened, plugged again, and then reopened. The results of the present study provide evidence that the vent of Capsule 48 may have been plugged. Capsules 44 and 49 had extensive deposits and could have been or did become plugged. The microprobe work of the present study suggests that the intermittent gas release from the vents is caused by formation of a liquid phase in the filter element. According to this hypothesis, the liquid phase could accumulate until it filled the vent and blocked release of decay helium. The internal pressure could then build up until it blew a channel through the liquid phase and vented the helium. The present study shows that vent plugging is a function of the impurities in the fuel and the possibility of this occurrence might be minimized by reducing the impurities in the fuel. This study also provides evidence that vent plugging may possibly be prevented by increasing the oxygen activity. Hence, the present work suggests that vacuum outgassing of pellets as a final heat treatment may not be as beneficial as originally expected.

Another major concern of Ir/PuO_2 compatibility is the effect of aging at elevated temperatures on the mechanical properties of the DOP-26 Ir. The present study confirms that aging Ir in the presence of PuO_2 leads to enhanced grain growth over aging of the Ir alone, especially of near-surface-grains (NSG) next to the fuel. Vent cups were especially susceptible to exaggerated grain growth. ORNL[4] has established that a major mechanism for grain growth is loss of Th from the Ir by oxidation of the Th at the surface. For exaggerated growth of the near-surface-grains (NSG) like that seen in the cups of this study during aging for six months at 1330°C, an oxygen pressure of 10^{-5} torr was necessary to remove enough Th to cause the exaggerated grain growth. The present study also shows evidence correlating growth of the NSG to loss of Th. Other effects may contribute to grain growth, but assuming Th depletion to be the primary cause, a key question to answer is the mechanism by which the fuel leads to Th depletion in the Ir. It is evident from the control samples of this study that the oxygen pressure was less than 10^{-5} torr since very little growth of the NSG was observed. It is expected that the graphite containers in which the samples were aged would maintain an oxygen pressure of about 10^{-9} torr at 1310°C Ir temperature. If the Th loss is due to oxygen pressure, then it is evident that the partial pressure of oxygen above the fuel within the capsule is greater than the partial

pressure of oxygen outside the capsule. The results of the compatibility study also indicate that grain growth was greater for Capsule 49 which had much higher levels of impurities in the fuel. This would suggest that the impurities raised the internal oxygen pressure in the capsule if reaction with the Th at the Ir surface is controlled by oxygen pressure. However, Liu[5] suggests that diffusion of the Th to the surface along grain boundaries, not oxygen pressure, is reaction rate controlling at the oxygen pressures expected in the capsule. If this is true, then the action of the impurities such as Fe and Cr which were found in large amounts on the grain boundaries may be to enhance Th diffusion. On the other hand, the impurities on the grain boundaries may act independently of the Th to cause grain growth by some mechanism such as changing interfacial energies.

The change in grain boundary chemistry observed in this study is expected to have some effect on impact ductility of the Ir apart from questions of grain size. The addition of Fe and Cr to the grain boundaries and the loss of Al associated with that addition is bound to have some affect on grain boundary cohesion and dislocation motion. However, how the ductility has been changed is not known.

The results of the Ir/Pu compatibility study also show that the impurities in the fuel have the following effects:

- Enhanced Pu escape from the CVS.
- Enhanced possibility of Ir crack initiation near the vent hole through formation of brittle Ir-Si intermetallics and very large grains (one to two grains per thickness).
- P levels normally present in the fuel show no evidence of producing deleterious effects in the fueled clads. We feel that phosphorus concentration in the fuel should not exceed about 15 ppm.

RECOMMENDATIONS

The results of this study lead to several recommendations which should be considered by the heat source community for future research and production programs. Implementation in the current program is not possible because production of fuel is almost completed. Impurity reduction has not been shown to significantly enhance fuel quality, but may be desirable in the future to further ensure reliability.

Even though the GPHS fuel is expected to perform acceptably, the present study demonstrates that impurities in the fuel can affect the performance of the CVS. Hence, it is recommended that Ca, Al, and especially Si concentrations in the fuel be reduced to as low as practical in future heat source programs. To do this in

the short term and to minimize the effects of the impurities that remain in the fuel, it is felt that the current final heat treatment in oxygen and vacuum outgassing steps could be reversed. This recommendation would have to be tested before implementation. The new regimen would have the pellets be vacuum outgassed for 6 hours at 1500°C and then heat treated in oxygen at 700°C for approximately two hours (the exact time to be determined). The current specifications for Si, Ca, and Al for the PuO_2 feed are: Si, 200 ppm; Ca, 300 ppm; Al, 150 ppm. The measured concentration of these elements are typically less than 100 ppm. Since concentrations of a few hundred ppm of these elements show signs of second phase formation in the fuel (HF-2 from ECT-1 and Pellet 49 from the current study) which leads to vent plugging, a reduction in impurity level would be desirable. Fueled capsules for which the PuO_2 has a Ca, Al, or Si content greater than about 100 ppm could cause problems. These capsules could have large quantities of deposits in the vents if they have been stored at elevated temperatures for several months. For the longer term, we recommend that a cost/benefit study be made on ways to reduce these elements to the lowest practical level. Since the actual levels to which these impurities should be reduced is not known, it is recommended that a study of the thermochemistry of these impurities in the PuO_2/Ir system be made. This study would identify the vapor species and vapor pressure of these species at different temperatures and oxygen activities as a function of storage time. These results would then be correlated with the observed build up of deposits in vents of CVS's heated under controlled conditions of temperature and oxygen activity (for example, with and without vacuum outgassing). As part of this work the reaction between Th and impurity vapor species would be investigated to help understand the cause of the Th depletion observed in the present study.

Fe, Cr, and Ni migrate from the fuel to the Ir cladding and alter the chemistry of the near-surface-grains and grain boundaries. Although the effect of these impurities is not now known, they should probably be excluded from the iridium until their effect is understood. The current specification for these impurities in the fuel is relatively high: Fe, 800 ppm; Cr, 250 ppm, Ni, 150 ppm. Although the compatibility study did not provide information on what the maximum concentration of these impurities in the fuel should be, it is felt that they should be as low as practical. We recommend that additional work be performed to establish the effect of different concentrations of Fe, Cr, and Ni on the impact ductility of DOP-26 Ir. These tests should specifically study the interactions of Th with Fe and Cr. If the test showed these elements degrade the iridium, then further work should be directed at determining the maximum concentration of these elements permissible in the fuel in order to maintain the impurity level in the Ir below the critical value.

The PuO_2 currently produced by SRP is optimum for the existing equipment and process. Any significant reduction in impurity level in future programs will require extensive studies in precipitation chemistry and powder processing. A capital investment program in processing equipment will be necessary. In order to make a reduction in impurities program meaningful, improved analytical techniques and equipment will have to be available for future heat source programs.

REFERENCES

1. C. T. Liu and H. Inouye. "Development and Charaterization of an Improved-Ir-0.3% W Alloy for Space Radioisotopic Heat Source." ORNL Report 5290 (October 1977).

2. C. A. Alexander, J. S. Ogden, and W. M. Pardue. "Mass Transport Within the Encapsulated MHW Fuel." Battelle Columbus Laboratory, July 13, 1973.

3. "Pu-238 Fuel Form Processes Quarterly Report, July - September 1982." USDOE Report DPST-82-128-3, E. I. du Pont de Nemours & Company, Savannah River Laboratory, Aiken, SC (1982).

4. C. L. White and C. T. Liu. "Outward Diffusion, and External Oxidation of Thorium in Iridium Alloys." Acta Met., Vol 29, pp. 301-310 (August 1980).

5. Private Communication, C. T. Liu (ORNL) to D. H. Taylor (SRL).

TABLE 1

Test Matrix for Ir/PuO_2 Compatibility Test

Sample Number	SRL Run No.	Phosphorus Concentration	Cation Concentration		Vacuum Outgassing
			Ca, Al, Si	Fe	
1	44	Background (∿5 ppm)	Background (30-50 ppm)	Background (∿1000 ppm)	Yes
2	48	20-30 ppm	Background (50-200 ppm)	Background (∿7,000 ppm)	Yes
3	49	7-40 ppm	100-1,000 ppm	Background (70-10,000 ppm	Yes
4	45	Background (∿4 ppm)	Background (50-200 ppm)	Background (800-2,000 ppm)	No

TABLE 2

Test Conditions

Aging temperature	GPHS-RTG iridium operating temperature - 1310°C (maximum fuel temperature approximately 1441°C)
Aging time	6 months
Aging atmosphere	Vacuum (about 1 x 10^{-6} torr)

TABLE 3

Chemistry of PuO_2 Fuel Before and After Aging as Measured by Spark Source Mass Spectroscopy (SSMS)

Concentration given in weight ppm.

Key to Table

Surf = Sample taken near pellet surface

Core = Sample taken from core region of pellet

H.T. = Pellet heat treated for 6 hours at 1525°C in oxygen

V/O = Pellet heat treated as above followed by vacuum outgassing for 1 hr at 1500°C

Aged = Pellet aged for 6 months in vacuum at about 1441°C (fuel temperature)

Element	44 Surf			44 Core			45 Surf		45 Core	
	H.T.	V/O	Aged	H.T.	V/O	Aged	H.T.	Aged	H.T.	Aged
Al	20	30	5	30	30	10	50	3	60	10
B			0.4			0.4		<0.01		<0.02
Ca	2	2	6	2	2	10	4	0.3	3	7
Cl			8			10		5		2
Co			2			0.7		<0.3		<0.2
Cr			70			20		20		10
Cu			4			2		2		0.7
Fe	1,000	1,000	300	900	900	100	800	100	2,000	70
K			0.4			0.8		0.7		0.05
Mg			1			1		0.7		0.5
Mn			30			10		5		8
Mo			4			3		1		0.5
Na			1			1		0.5		0.2
Ni			40			10		5		7
P	5	6	0.5	7	4	0.5	3	0.2	4	0.1
S	30	20	40	20	20	30	20	30	20	40
Si	40	50	10	100	40	20	200	10	100	7
Th			700			2,000		300		400
V			0.3			<0.2		<0.1		0.1
Ti			3			3		4		3

TABLE 3, Contd

Element	48 Surf			48 Core		
	H.T.	V/O	Aged	H.T.	V/O	Aged
Al	70	200	50	70	60	200
B			0.1			0.1
Ca	50	100	4	70	50	40
Cl			8			20
Co			1			2
Cr	500	1,000	50	1,000	1,000	100
Cu			2			10
Fe	~2,000	~7,000	200	~5,000	~7,000	400
K			0.3			1
Mg	2	3	3	2	2	7
Mn			20			60
Mo			4			20
Na			1			4
Ni	500	800	20	400	900	40
P	200	20	50	200	30	50
S	20	10	60	10	10	100
Si	300	100	50	200	100	400
Th			200			300
V			<0.2		<0.5	
Ti	≤3	≤4	10	≤3	≤3	20

TABLE 3, Contd

Element	49 Surf			49 Core			Efflusate From Vent of Capsule 49
	H.T.	V/O	Aged	H.T.	V/O	Aged	
Al	∿3,000	200	∿300	>3,000	900	∿1,000	∿2,000
B			0.1			0.1	<1
Ca	1,000	100	100	2,000	600	300	∿4,000
Cl			10			10	50
Co			0.1			0.2	1
Cr	300	30	2	500	2,000	7	10
Cu			0.2			0.1	3
Fe	2,000	70	5	∿3,000	∿10,000	10	30
K			0.3			0.1	0.1
Mg	2	≤0.7	<0.3	3	4	2	<1
Mn			0.6			2	1
Mo			<0.5			1	6
Na			4			10	<1
Ni	400	7	0.6	500	2,000	0.7	2
P	∿1,000	7	5	∿1,000	40	20	4
S	10	10	20	30	20	30	9
Si	2,000	200	∿500	3,000	1,000	∿2,000	100
Th			300			200	15,000
V			<0.1			<0.03	<1
Ti	≤3	<0.5	1	≤3	5	2	900
Au							<10
Ba							10
Ce							4
Ir							∿20,000
Ta							200
W							∿8,000
Sr							10
Pu-239							major
Pu-238							major
Pu-240							20,000
Pu-241							5,000
Pu-242							400
U-234							4,000
Np-237							200

TABLE 4

Current Specifications for Impurities in GPHS Fuel (DPST-79-1076)

Element	Wt, ppm
Al	150
B	1
Ca	300
Cd	50
Cr	250
Cu	100
Fe	800
Mg	50
Mn	50
Mo	250
Na	250
Ni	150
Pb	100
Si	200
Sn	50
Zr	50
Ti	No specification
Actinides	
Am U Th Np	$\leq$1%

No individual impurity is to exceed 1/2% by weight.

TABLE 5

Summary of PuO_2 Chemistry Comparing Results of Spark Source Mass Spectroscopy (SSMS) and Emission Spectroscopy (ES) for Major Impurities

Double entries for SSMS data refer to values for surface and core samples. Values are weight ppm.

Element	Pellet 44			Pellet 45		
	SSMS		ES	SSMS		ES
	V/O	Aged	Aged	HT	Aged	Aged
Al	30/30	5/10	60	50/60	3/10	60
Ca	2/2	6/10	15	4/3	0.3/7.0	15
Cr		70/20	<5		20/10	6
Fe	1000/900	300/100	30	800/2000	100/70	20
Mg		1	<1		7/5	<1
Ni		40/10	<5		0.5/0.2	<5
P	6/4	0.5/0.5	5*	3/4	0.2/0.1	5*
S	20/20	40/30	-	20/20	30/40	-
Si	50/40	10/20	35	200/100	10/7	30
Ti		3/3	10		4/3	7

Element	Pellet 48			Pellet 49		
	SSMS		ES	SSMS		ES
	V/O	Aged	Aged	V/O	Aged	Aged
Al	200/60	50/200	65	200/900	300/1000	190
Ca	100/50	40/40	15	100/600	100/300	200
Cr	1000/1000	50/100	9	30/2000	2/7	<5
Fe	7000/5000	200/400	25	70/10,000	5/10	7
Mg	3/2	3/7	<1	<7/4	<3/2	<1
Ni	800/900	20/40	<5	7/2000	0.6/0.7	<5
P	20/30	50/50	20*	7/40	5/20	35*
S	10/10	60/100	-	10/20	20/30	-
Si	100/100	50/400	50	200/1000	500/2000	170
Ti	<4/<3	10/20	10	<0.5/5	1/2	8

* Determined by colorimetry at LANL.

TABLE 6

Average Grain Size of Iridium

Comparison of Pre-Aged, Aged but Unfuel, and Aged and Fueled Iridium

Grain size measured axially 100 μm from surface next to fuel (interior), along center line of iridium thickness (center), and 100 μm from surface next to graphite (exterior). Measurements made on several photomicrographs to improve statistics.

Grain size given in micrometers, μm.

		Archive Rings (Unfueled Control Samples)				Cups (Fueled Iridium)		(Unfueled)	
		Pre-Aged		Aged		Aged		Aged	
Location	Pellet Number	Vent*	Shield**	Vent	Shield	Vent	Shield	A	B
Exterior	44	46	46	72	66	110	100		
	45	42	55	56	71	87	111		
	48	58	39	82	53	301	107		
	49	79	54	90	78	126	115		
Average		56	49	75	67	156	108	72	64
Center	44	38	51	68	65	72	66		
	45	37	44	50	66	82	101		
	48	51	37	74	57	91	88		
	49	54	41	79	74	90	104		
Average		45	43	68	66	84	90	63	65
Interior	44	43	47	56	57	167	197		
	45	50	58	50	89	182	138		
	48	54	68	72	64	188	128		
	49	77	39	73	53	217	131		
Average		56	53	63	66	189	149	82	71
Overall Average		52	48	69	66	143	116	72	67

* Refers to archive ring from vent cup (cup having vent hole) used to encapsulate given pellet.

** Refers to archive ring from shield cup (cup having welding shield) used to encapsulate given pellet.

TABLE 7

Comparison of Grain Size of Iridium Cups from Each Fuel Pellet, μm

Thorium content (expressed as Th_{65}/Ir_{229} auger peak height ratios) are included for reference.

Location on Iridium Cross Section	Pellet 44		Pellet 45		Pellet 48		Pellet 49	
	Grain Size	$\frac{Th_{65}}{Ir_{229}}$	Grain Size	$\frac{Th_{65}}{Ir_{229}}$	Grain Size	$\frac{Th_{65}}{Ir_{229}}$	Grain Size	$\frac{Th_{65}}{Ir_{229}}$
Vent Cups								
Exterior	110	0.43	87	0.57	301	0.40	126	0.46
Center	72	0.59	82	0.65	91	0.43	90	0.64
Interior	167	0.33	182	0.24	188	0.0	217	0.21
Average	116	0.45	117	0.49	193	0.28	144	0.44
Shield Cups								
Exterior	100	0.46	111	0.27	107	0.68	115	0.77
Center	66	0.74	101	0.69	88	0.49	104	0.61
Interior	197	0.41	138	0.31	128	0.61	131	0.56
Average	121	0.54	117	0.42	108	0.59	117	0.65
Average of Both Cups	119	0.50	117	0.46	151	0.44	131	0.51

Average Th for all cups = 0.48 ±0.11.

TABLE 8

Iridium Chemistry

Comparison of unaged and aged archive rings to aged fueled cups by Spark Source Mass Spectroscopy (SSMS), ppm. Analyses of selected aged fueled cups by Emission Spectroscopy (ES) is also included. Dash (-) indicates no data.

	Pellet 44: Vent Cup				Pellet 44: Shield Cup				
	Archive Ring			Cup by	Archive Ring			Cup by	Pellet 44
Element	Unaged L-256-8	Aged	Cup	ES	Unaged L-254-7	Aged	Cup	ES	Weld
Al	27	24	53		15	29	60		38
B	0.1	<0.01	<0.01		0.01	<0.01	<0.01		<0.01
Ca	1	1	2		0.4	0.7	0.7		0.8
Co	-	<0.03	0.3		-	<0.05	0.2		<0.05
Cr	0.7	0.4	0.5		0.3	2	5		1
Cu	7	1	2		3	2	2		1
Cl	-	0.5	0.05		-	0.1	0.2		0.2
Fe	6	7	10		10	20	30		20
Ir	M	M	M		M	M	M		M
K	-	0.5	0.1		-	0.1	0.2		0.1
Mg	-	<0.05	<0.3		-	0.1	<0.09		<0.03
Mn	-	0.03	0.1		-	3	0.2		0.07
Mo	≤0.5	7	1		1	0.5	1		1
Na	0.1	0.4	0.3		0.05	0.07	0.3		0.3
Ni	≤0.5	<0.2	0.8		2	0.5	3		4
P	0.02	0.04	0.1		0.03	<0.03	0.1		0.03
Pt	≤1	<2	<3		≤5	20	<3		<2
Re	-	<1	<1		-	20	10		10
Rh	0.6	0.6	0.7		0.8	0.5	0.7		0.7
Ru	7	5	8		3	7	6		7
S	2	3	7		2	3	7		4
Si	1	2	5		1	1	7		2
Ta	≤20*	-	-		≤40*	-	-		-
Th	50	39	57		36	45	48		36
Ti	≤0.2	-	-		≤0.3	-	-		-
V	-	<0.1	0.3		-	0.1	0.2		<0.1
W	2,800	3,800	5,900		2,500	2,000	7,700		3200
Zr	0.1	-	-		0.2	-	-		-

* Source made from Ta.

TABLE 8, Contd

Element	Pellet 45: Vent Cup Archive Ring Unaged L-257-R2	Aged	Cup	Cup by ES	Pellet 45: Shield Cup Archive Ring Unaged L-255-6	Aged	Cup	Cup by ES	Pellet 45 Weld
Al	43	45	48		10	36		150	170
B	0.02	0.01	<0.01		0.02	<0.01		<10	<0.01
Ca	1	0.7	0.7		0.5	0.7		<3	1
Co	-	<0.03	<0.3		-	<0.03		<10	0.2
Cr	3	0.4	3		0.5	0.3		20	8
Cu	40	2	2		2	1		10	5
Cl	-	0.05	0.2		-	0.1		-	0.1
Fe	20	3	5		2	2		300	40
Ir	M	M	M		M	M		M	M
K	-	0.1	0.3		-	0.1		<3,000	0.3
Mg	-	<0.05	<0.03		-	<0.02		3	<0.1
Mn	-	0.1	<0.05		-	<0.05		<30	0.3
Mo	≤0.5	1	0.7		1	0.7		<200	0.7
Na	0.05	0.07	1.4		0.1	0.1		<300	1
Ni	1	0.2	1		≤0.3	0.3		40	3
P	0.03	<0.01	0.1		0.02	<0.02		<300	0.2
Pt	≤5	<4	<2		≤5	<2		<30	<2
Re	-	<1	5		-	4		-	7
Rh	0.5	0.5	0.5		1	0.7		<30	1
Ru	5	4	4		10	7		<30	7
S	6	4	3		2	3		-	5
Si	2	1	6		5	<1		<10	20
Ta	≤50*	-	-		≤10*	-		<1,000	-
Th	60	70	40		20	75		-	52
Ti	≤0.2	-	-		≤0.1	-		<30	-
V	-	0.3	<0.1		-	<0.1		<30	<0.2
W	3,100	3,800	2,700		2,900	2,900		1,000-10,000	3,600
Zr	0.2	-	-		0.1	-		<200	-

* Source made from Ta.

TABLE 8, Contd

Element	Pellet 48: Vent Cup Archive Ring Unaged P-701-4	Aged	Cup	Cup by ES	Pellet 48: Shield Cup Archive Ring Unaged N-502-3	Aged	Cup	Cup by ES	Pellet 48 Weld
Al	26	28	49	70	34	21		50	47
B	≤0.02	<0.01	<0.01	<10	0.02	<0.01		<10	<0.01
Ca	1	0.4	1	<3	0.5	0.7		3	1
Co	-	<0.03	<0.05	-	-	<0.03		<10	<0.05
Cr	1	0.2	2	<10	0.7	0.5		<10	-
Cu	3	1	1	5	3	3		15	3
Cl	-	0.05	0.1	-	-	0.07		-	<0.05
Fe	2	1	10	150	3	3		170	10
Ir	M	M	M	-	M	M		M	M
K	-	0.1	0.07	<3,000	-	0.08		<3,000	0.1
Mg	-	<0.04	<0.02	<3	-	<0.01		<3	<0.02
Mn	-	0.05	0.2	<10	-	0.07		<10	<0.1
Mo	0.3	0.5	0.7	<200	≤0.5	3		<200	1
Na	0.4	0.1	0.2	<300	0.05	0.05		<300	0.2
Ni	1	0.1	2	10	0.3	0.4		20	0.7
P	0.05	<0.02	0.06	<300	0.02	<0.01		<300	0.04
Pt	≤7	<2	<3	<30	≤1	<1		<30	<2
Re	-	<1	<2	-	-	<1		-	<1
Rh	<0.05	0.4	0.7	<30	1	0.5		<30	<0.5
Ru	<0.3	1	1	<30	10	3		<30	6
S	6	1	3	-	2	2		-	3
Si	≤2	<1	7	10	≤1	<1		5	7
Ta	≤5*	-	-	<1,000	≤20*	-		<1,000	-
Th	27	43	36	-	53	35		-	41
Ti	≤0.2	-	-	<30	≤10	-		<30	-
V	-	<0.1	<0.3	<30	-	<0.06		<30	0.3
W	2,800	2,600	3,900	1,000-10,000	3,100 -	2,900		1,000-10,000	2,900
Zr	0.2	-	-	<200	0.1	-		<200	-

* Source made from Ta.

TABLE 8, Contd

Element	Pellet 49: Vent Cup Archive Ring Unaged P-714-5	Aged	Cup	Cup by ES	Pellet 49: Shield Cup Archive Ring Unaged PR-715-2	Aged	Cup	Cup by ES	Pellet 49 Weld
Al	27	46	56	80	48	15	75	60	45
B	0.01	<0.01	<0.01	<10	0.01	<0.01	<0.01	<10	<0.01
Ca	0.3	0.7	2	<3	0.7	0.5	3	3	1
Co	-	<0.06	<0.04	-	-	<0.03	0.2	-	<0.07
Cr	0.8	5	1	40	0.3	0.5	3	40	2
Cu	2	4	3	10	5	2	4	15	3
Cl	-	0.3	0.3	-	-	0.2	0.2	170	0.07
Fe	7	20	10	300	2	5	20	-	10
Ir	M	M	M	-	M	M	M	M	M
K	-	0.1	0.1	<3,000	-	0.07	0.3	<3,000	0.1
Mg	-	<0.1	<0.04	<3	-	<0.05	<0.03	<3	<0.05
Mn	-	0.3	0.5	<10	-	0.08	0.2	<10	0.2
Mo	≤0.5	0.5	0.7	<200	≤0.1	1	0.7	<200	<0.5
Na	0.1	0.1	0.3	<300	0.07	0.07	0.5	<300	2.4
Ni	0.7	0.5	0.7	40	0.1	0.3	1	30	0.7
P	0.03	0.04	0.07	<300	0.01	<0.03	0.7	<300	0.1
Pt	≤7	<2	<2	<30	≤2	<3	<2	<30	<2
Re	-	<1	<1	-	-	<1	<1	-	<1
Rh	2	0.1	<0.1	<30	≤0.05	0.4	0.3	<30	<0.2
Ru	<0.5	<0.5	0.7	<30	≤0.4	5	2	<30	1
S	2	5	5	-	3	3	5	-	4
Si	2	1	8	10	≤0.7	<0.05	7	7	7
Ta	≤20*	-	-	<1,000	≤10*	-	-	<1,000	-
Th	46	55	52	-	65	34	55	-	59
Ti	≤0.2	-	-	<30	≤0.1	-	-	<30	-
V	-	<0.05	<0.1	<30	-	<0.07	0.2	<30	<0.07
W	3,200	1,900	2,700	1,000-10,000	3,600	2,400	3,600	1,000-10,000	3,900
Zr	0.3	-	-	<200	0.1	-	-	<200	-

* Source made from Ta.

TABLE 8, Contd

Element	Unfueled Capsule, T-40 A, Top Cup Archive Ring Unaged NR-520-2	Aged	Cup	Cup by ES	Unfueled Capsule, T-40 B, Bottom Cup Archive Ring Unaged PR-719-6	Aged	Cup	Cup by ES	T-40 Weld
Al	13	25	44		49	26	35		34
B	≤0.01	<0.01	<0.01		0.04	<0.01	<0.01		<0.01
Ca	1	0.5	1		5	0.7	0.8		1
Co	-	<0.04	0.03		-	<0.02	<0.04		<0.1
Cr	1	0.4	0.5		2	0.3	<0.5		2
Cu	10	3	4		20	3	3		4
Cl	-	0.1	0.2		-	0.07	0.3		0.7
Fe	10	3	2		10	1	4		7
Ir	M	M	M		M	M	M		M
K	-	0.2	0.08		-	0.1	0.1		0.3
Mg	-	<0.07	<0.05		-	<0.02	<0.05		<0.1
Mn	-	0.04	<0.02		-	0.05	<0.05		<0.05
Mo	≤1	1	1		10	0.5	2		4
Na	0.1	0.1	0.2		1	0.07	0.2		0.3
Ni	0.7	0.4	0.5		4	0.3	0.7		2
P	0.03	<0.03	0.4		0.05	<0.02	0.05		0.1
Pt	≤2	2	<0.5		≤10	<1	<2		<2
Re	-	<1	<1		-	<1	<1		<1
Rh	2	1	1		3	0.8	0.4		1
Ru	10	10	10		10	4	3		10
S	4	3	3		10	3	4		5
Si	2	2	3		10	1	3		3
Ta	≤20*	-	-		≤20*	-	-		-
Th	46	57	60		42	55	34		36
Ti	≤0.4	-	-		≤0.5	-	-		-
V		<0.1	0.2		-	<0.05	<0.05		<0.05
W	2,500	2,400	2,300		3,500	2,600	3,400		2500
Zr	0.1	-	-		3	-	-		-

* Source made from Ta.

TABLE 9

Thorium Content of Iridium Grain Boundaries

Comparison of Pre-Aged, Aged but Unfueled, and Aged and Fueled Iridium. Thorium content measured by Auger electron spectroscopy (AES) at LANL and expressed as Th_{65}/Ir_{229} peak height ratio. Electron beam spot size about 15 μm. Three readings were taken across the iridium cross-section; one at about 100 μm from each edge and one at the center.

		Archive Rings (Unfueled Control Samples)				Cups (Fueled Iridium)	
		Pre-Aged		Aged		Aged	
Location	Pellet Number	Vent*	Shield**	Vent	Shield	Vent	Shield
Exterior	44	0.80	0.70	0.74	0.88	0.43	0.46
	45	0.55	0.87	0.90	0.66	0.57	0.27
	48	0.75	0.64	0.64	0.82	0.40	0.68
	49	0.73	0.66	0.87	0.81	0.46	0.77
	T-40†	0.71	0.65	0.70	0.84	(0.77††)	(0.67††)
Average		0.71	0.70	0.77	0.80	0.47	0.55
		σ = 0.09	σ = 0.10	σ = 0.11	σ = 0.08	σ = 0.07	σ = 0.22
Center	44	0.66	0.88	0.87	0.97	0.59	0.74
	45	1.08	0.96	0.88	1.03	0.65	0.69
	48	0.84	0.91	0.86	0.61	0.43	0.49
	49	0.68	0.84	0.71	1.01	0.64	0.61
	T-40†	0.78	0.94	0.85	1.13	(0.88††)	(0.74††)
Average		0.81	0.91	0.83	0.95	0.58	0.63
		σ = 0.17	σ = 0.05	σ = 0.07	σ = 0.20	σ = 0.10	σ = 0.11
Interior	44	0.80	0.78	0.66	0.44	0.33	0.41
	45	0.82	0.80	0.94	0.71	0.24	0.31
	48	0.57	0.60	0.69	0.84	-	0.61
	49	0.61	0.74	0.72	0.85	0.21	0.56
	T-40†	0.89	0.91	0.75	0.97	(0.73††)	(0.75††)
Average		0.74	0.77	0.75	0.76	0.20	0.47
		σ = 0.14	σ = 0.11	σ = 0.11	σ = 0.20	σ = 0.14	σ = 0.14
Overall Average		0.75	0.79	0.79	0.84	0.41	0.55
		σ = 0.13	σ = 0.12	σ = 0.10	σ = 0.18	σ = 0.19	σ = 0.16

* Refers to archive ring from vent cup used to encapsulate given pellet.

** Refers to archive ring from shield cup used to encapsulate given pellet.

† T-40 refers to unfueled capsule consisting of two shield cups welded together and aged in graphite as a further control sample.

†† Values in parentheses not included in column averge.

TABLE 10

Comparison of Grain Size Versus Thorium Content for Aged Iridium Cups

Location	Pellet Number	Vent Cups: Grain Size, μm	Vent Cups: Thorium Content, Th_{65}/Ir_{229}	Shield Cup: Grain Size, μm	Shield Cup: Thorium Content, Th_{65}/Ir_{229}	Capsule Average: Grain Size, μm	Capsule Average: Thorium Content, Th_{65}/Ir_{229}
Exterior	44	110	0.43	100	0.46	105	0.45
	45	87	0.57	111	0.27	99	0.42
	48	301	0.40	107	0.68	204	0.54
	49	126	0.46	115	0.77	121	0.62
Average		156	0.47	108	0.55	132	0.51
(T-40*)		(72)	(0.77)	(64)	(0.67)	(68)	(0.72)
Center	44	72	0.59	66	0.74	69	0.66
	45	82	0.65	101	0.69	91	0.67
	48	91	0.43	88	0.49	90	0.46
	49	90	0.64	104	0.61	97	0.63
Average		84	0.58	90	0.63	87	0.61
(T-40)		(63)	(0.88)	(65)	(0.74)	(64)	(0.81)
Interior	44	167	0.33	197	0.41	182	0.37
	45	182	0.24	138	0.31	160	0.28
	48	188	-	128	0.61	158	0.31
	49	217	0.21	131	0.56	174	0.39
Average		189	0.20	149	0.47	169	0.34
(T-40)		(82)	(0.73)	(71)	(0.75)	(77)	(0.74)
Overall Averages		143	0.42	116	0.55		

* T-40 = unfueled capsule.

TABLE 11

Qualitative Composition of Phases Identified in Vents

(Elements listed in apparent order of abundance)

Phase	Capsule	Elemental Composition
1	44, 45	Ca, Si, Mg, Pu, Al (contains Ca-Pu dendrites)
2	44, 45	Pu, O
3	44	Ca, Pu, O
4	44	Si, Mg, Ir
5	48	Ca, Pu, Mg, P, Si, O
6	48	Si, Mg, Ca, Pu
7	48	Ti, Al
8	49	Si, Ca, Al, Pu, O, P, Ti
9	49	Ca, P
10	44, 48, 49	Si, O
11	45, 48	Al, Ca, O, Pu
12	45	Ca, Al, O, Si, Pu
13	45	Ta, Ca, O, Al, Pu, Th. U, Si
14	49	Si, O, Pu, Ca, Al, Ti
15	44	Ca, Al, Pu, Si, O, Ti
16	44	Ca, Pu, Si, O
17	48	Ir, Si, Pu
18	48	Ir, Si, Pu, O
19	48	Pu, O, Al, Ca, Si
20	48	Cr, O, Fe, Mg, Al
21	49	Ir, Ti
22	49	Ir, Al

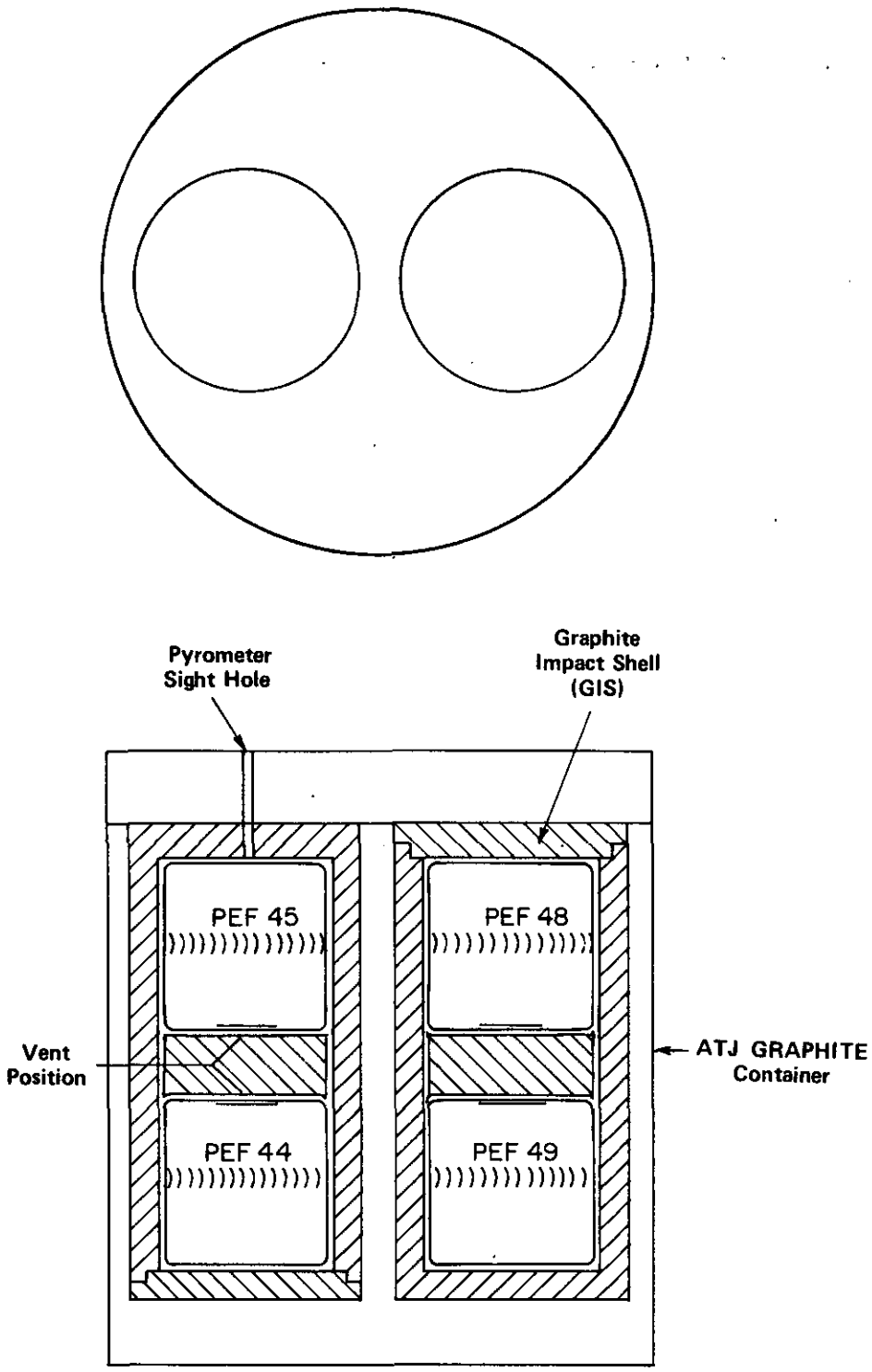

FIGURE 1. Orientation of Compatibility Test Pellets in Aging Furnace.

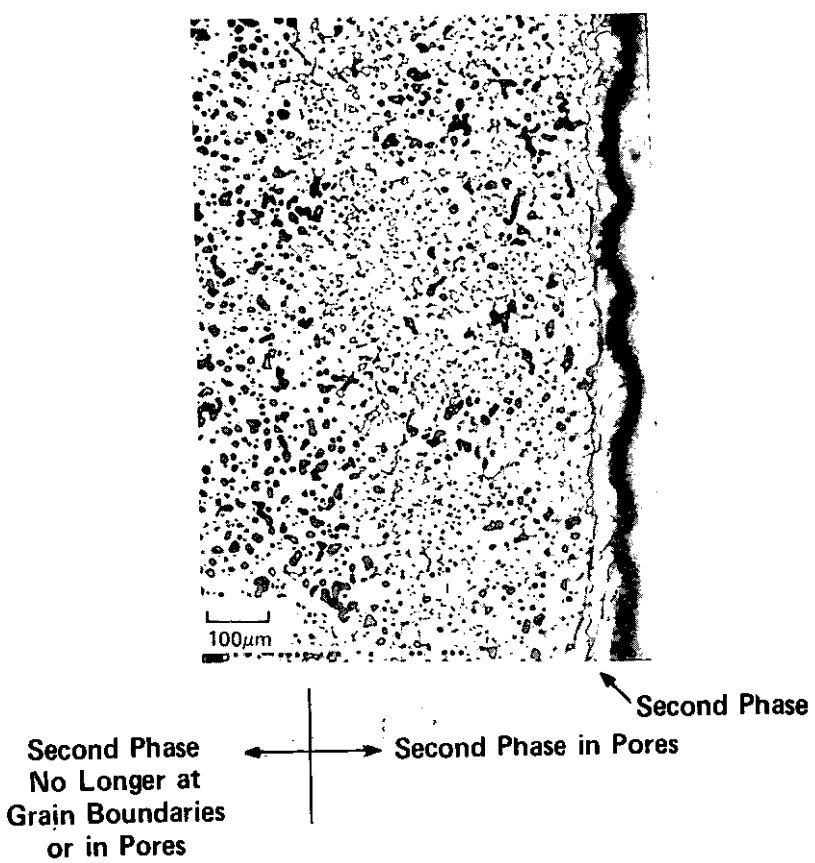

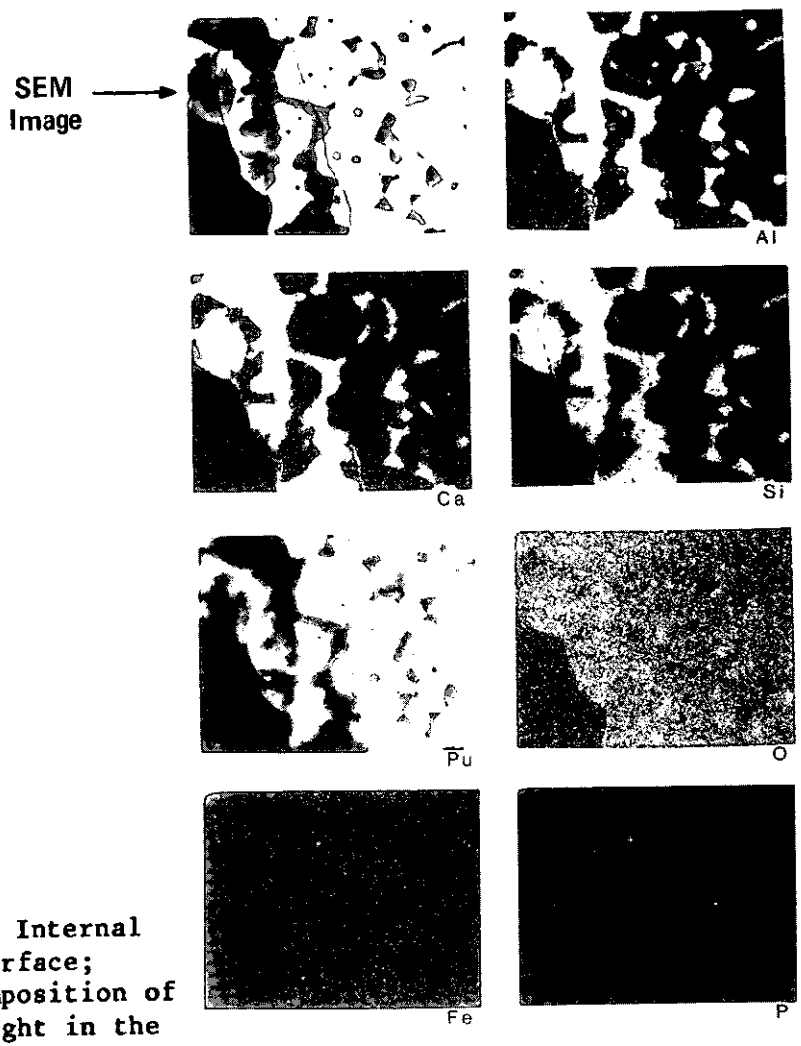

FIGURE 2. Pallet 49: (a) Second Phase (light gray) on Internal Crack Surface and in Pores Near the Crack Surface; (b) Microprobe Electron Dot Maps Showing Composition of Second Phase. The given element appears bright in the dot maps.

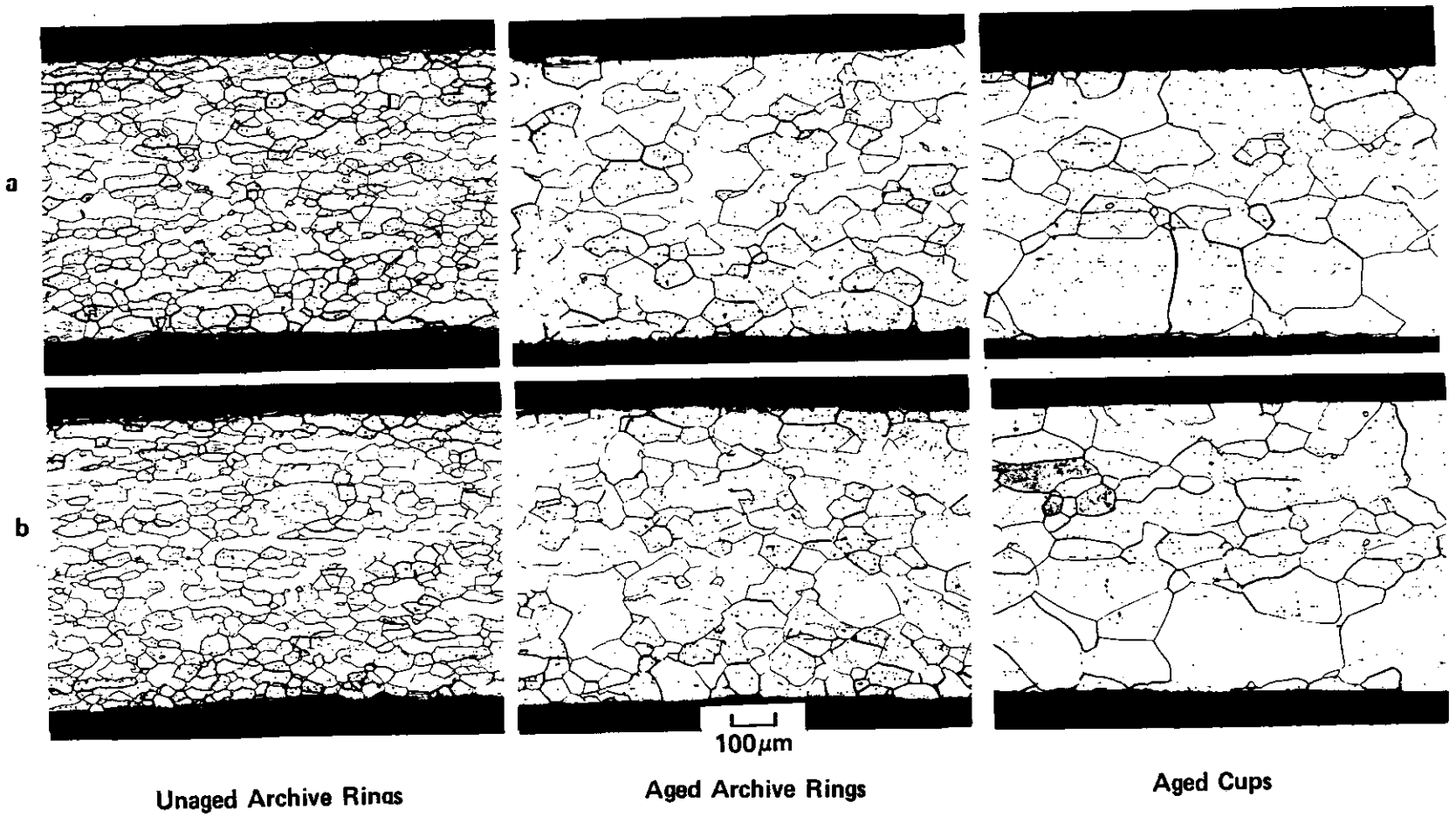

FIGURE 3. Capsule 44, Comparison or Unaged and Aged Archive Rings to Aged Fueled Iridium Clads: (a) Vent Cup (L 256-8); (b) Shield Cup (L 254-7). The bottom of each micrograph is the concave or interior surface (surface next to fuel for cups).

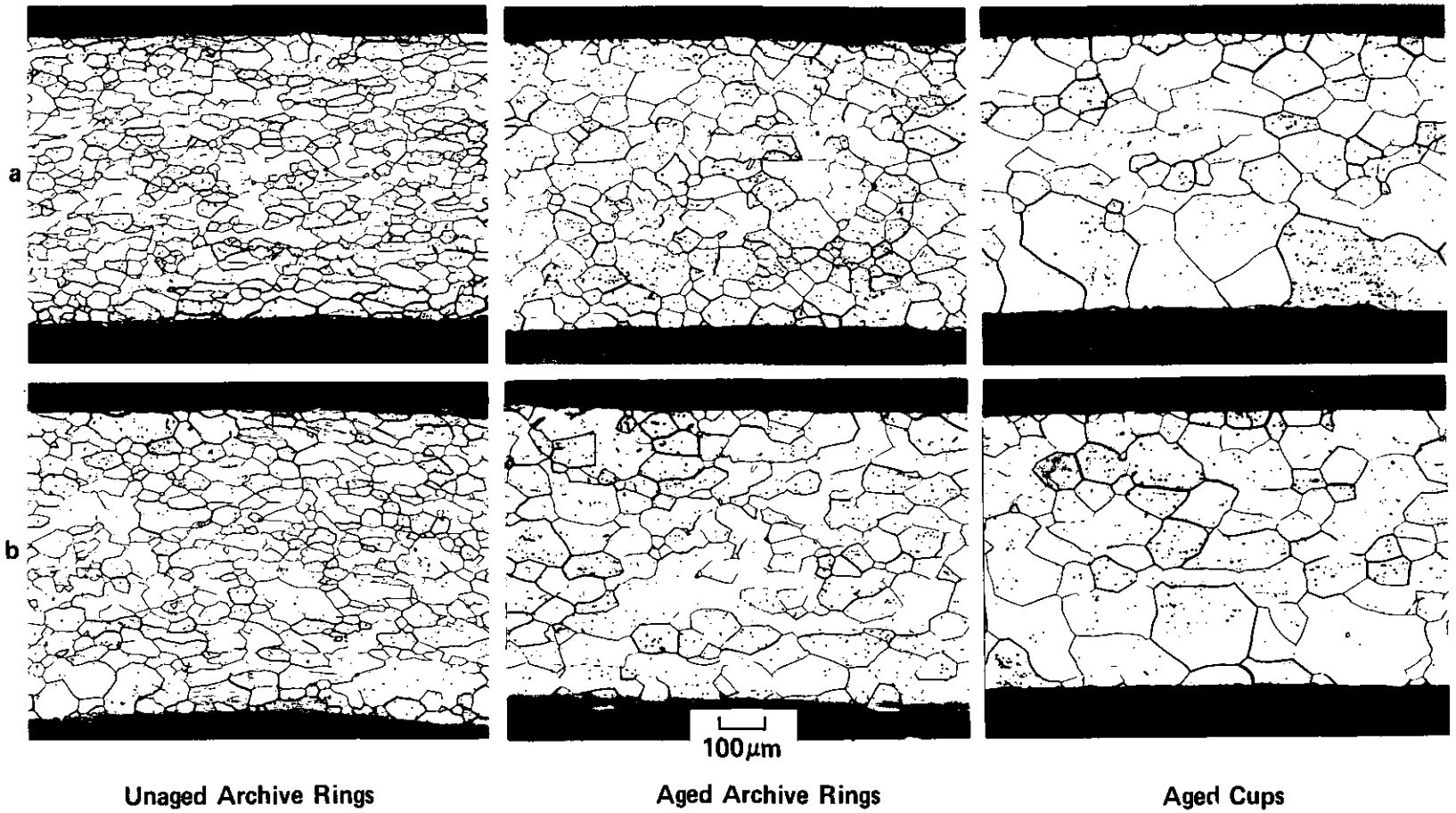

FIGURE 4. Capsule 45, Comparison of Unaged and Aged Archive Rings to Aged Fueled Iridium Clads: (a) Vent Cup (L 257-R2); (b) Shield Cup (L 255-6). The bottom of each micrograph is the concave or interior surface (surface next to fuel for cups).

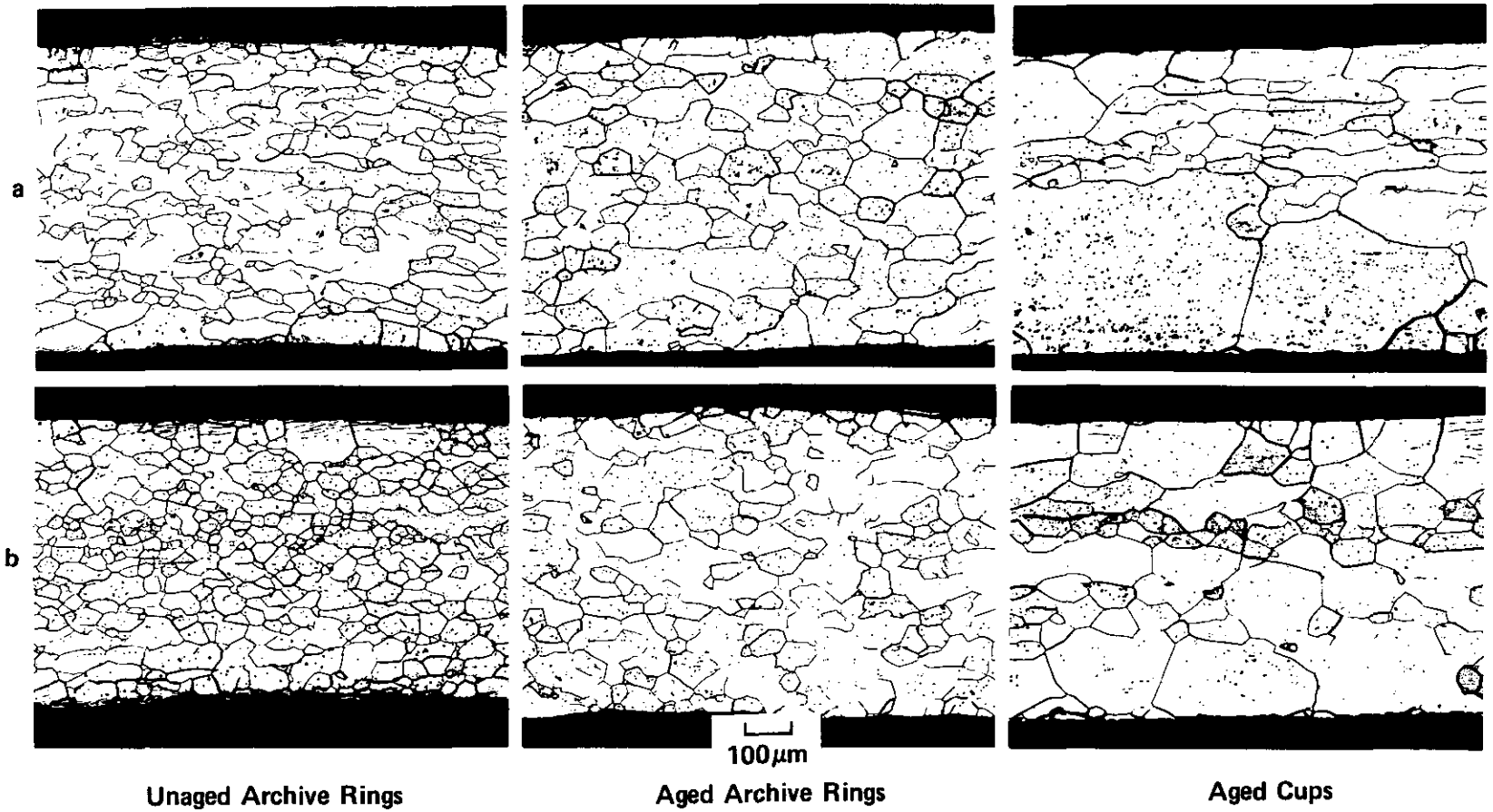

FIGURE 5. Capsule 48, Comparison of Unaged and Aged Archieve Rings to Aged Fueled Iridium Clads: (a) Vent Cup (P 701-4); (b) Shield Cup (N 502-3). The bottom of each micrograph is the concave or interior surface (surface next to fuel for cups).

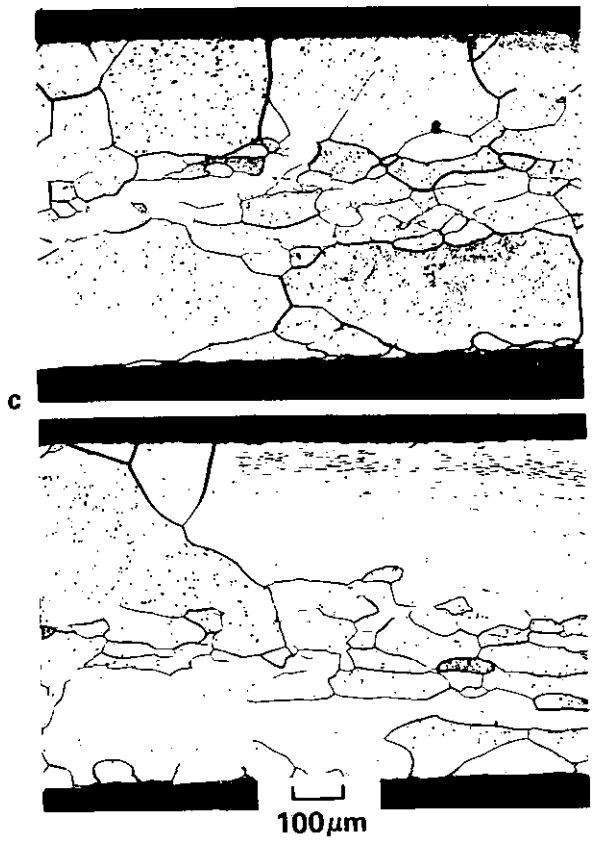

FIGURE 5. Capsule 48, Vent Cup Showing Areas of Large Grains at Continued Both the Exterior Edge (top of micrographs) and Interior Edge (bottom of micrographs).

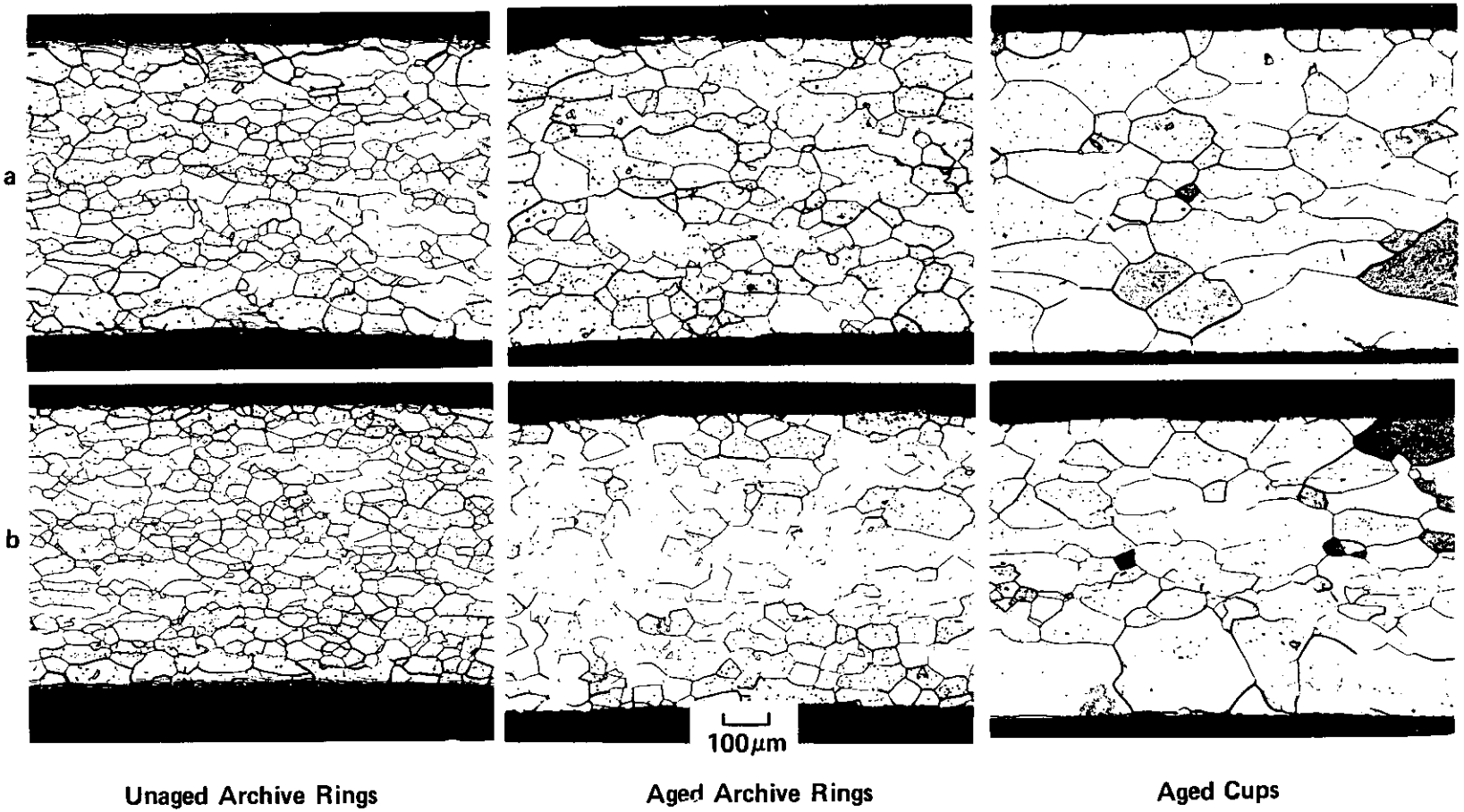

FIGURE 6. Capsule 49, Comparison of Unaged and Aged Archive Rings to Aged Fueled Iridium Clads: (a) Vent Cup (P 714-5); (b) Shield Cup (PR 715-2. The bottom of each micrograph is the concave or interior surface (surface next to fuel for cups).

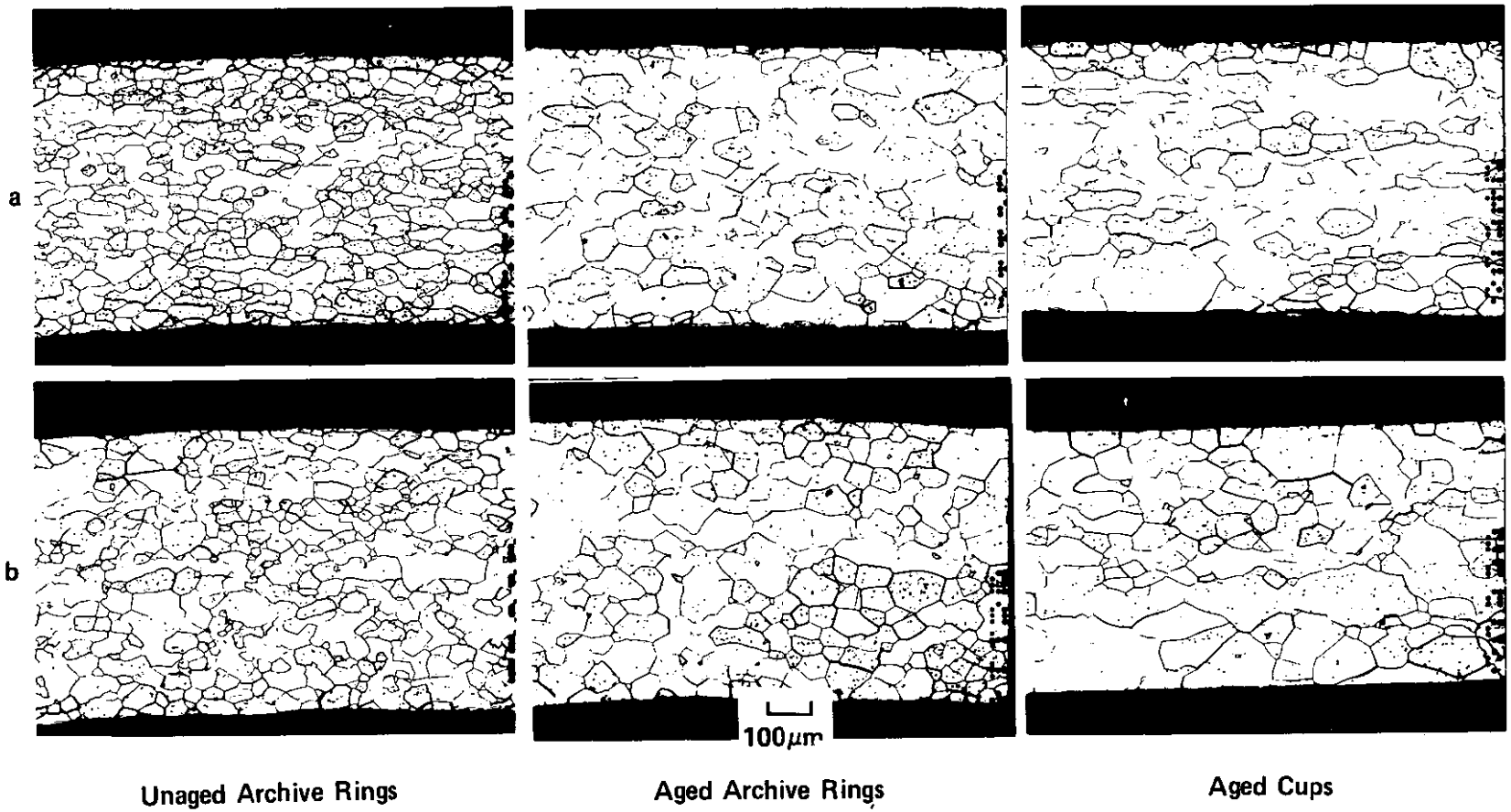

FIGURE 7. Capsule T-40 (Unfueled Control), Comparison of Unaged and Aged Archive Rings to Aged Iridium Clads: (a) Top Cup (NR 520-2); (b) Bottom Cup (PR 719-6). The bottom of each micrograph is the concave or interior surface.

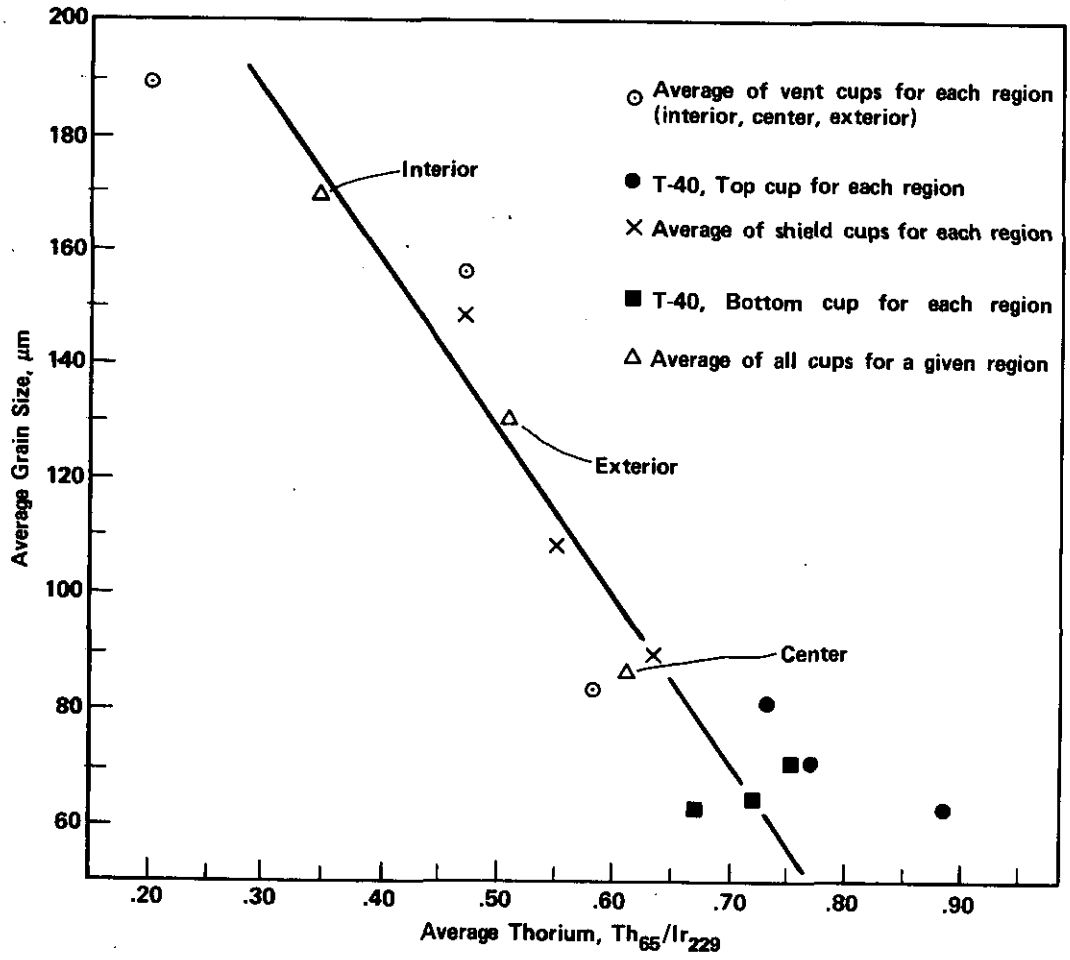

FIGURE 8. Average Thorium Content by AES Vs. Average Grain Size.

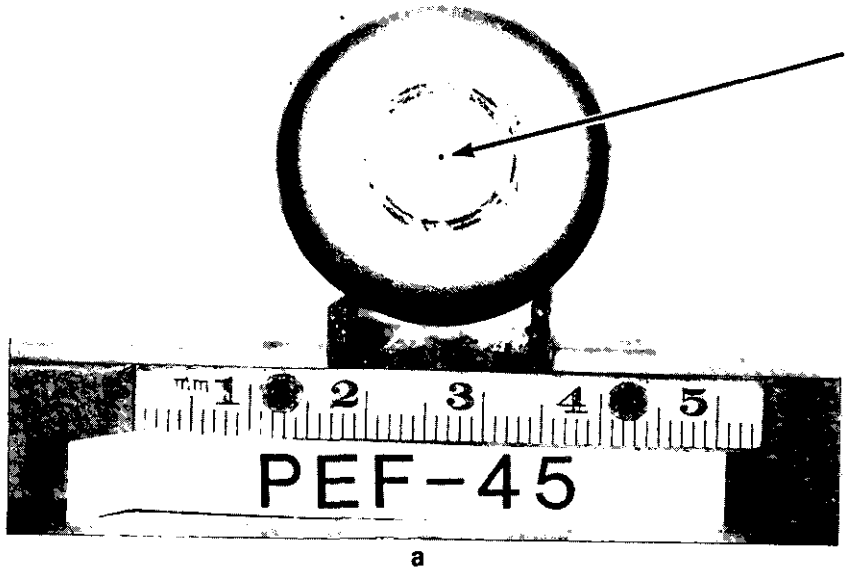

a

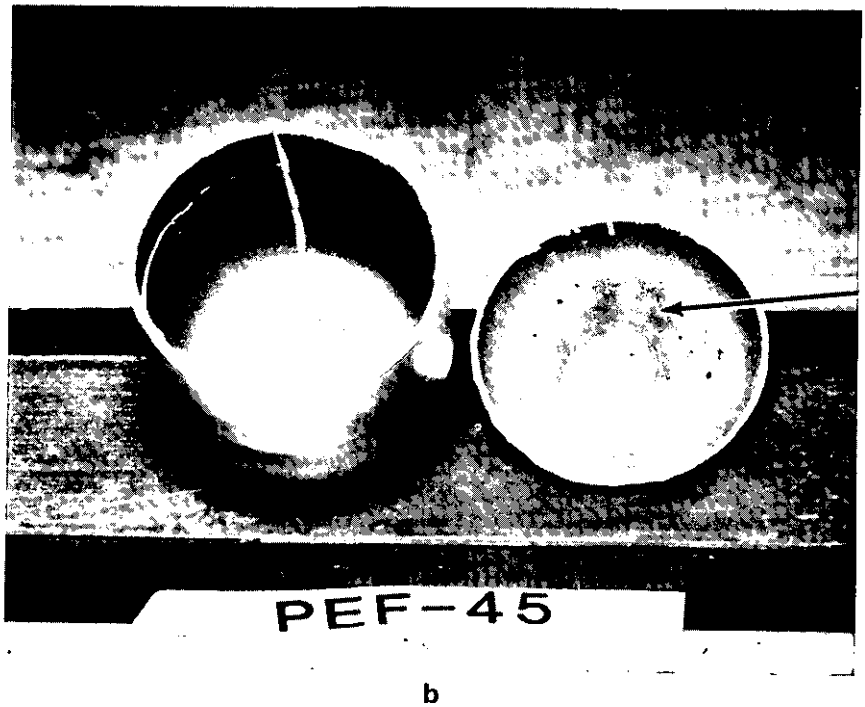

b

FIGURE 9. (a) Surface of Capsule 45 Showing Lack of Deposits Around Vent Hole; (b) Inner Surface of Cups.

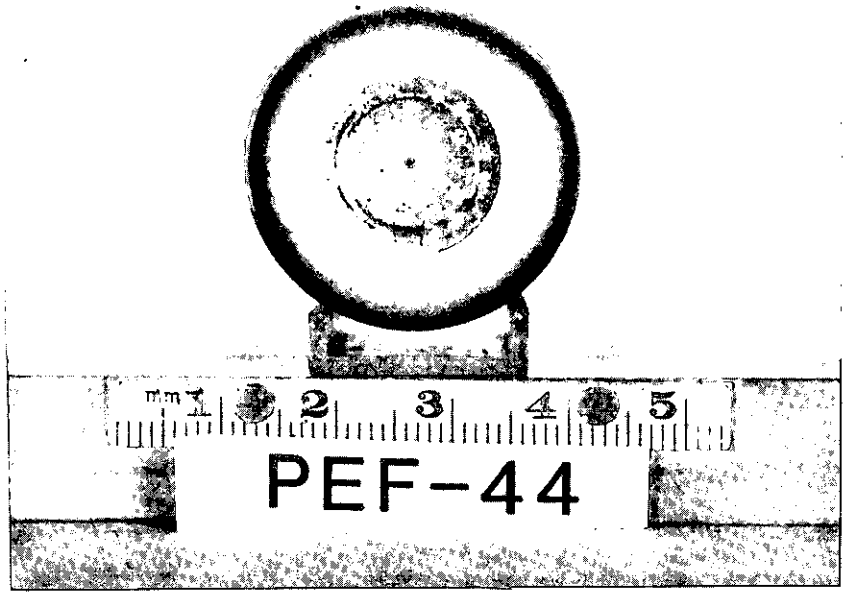

a

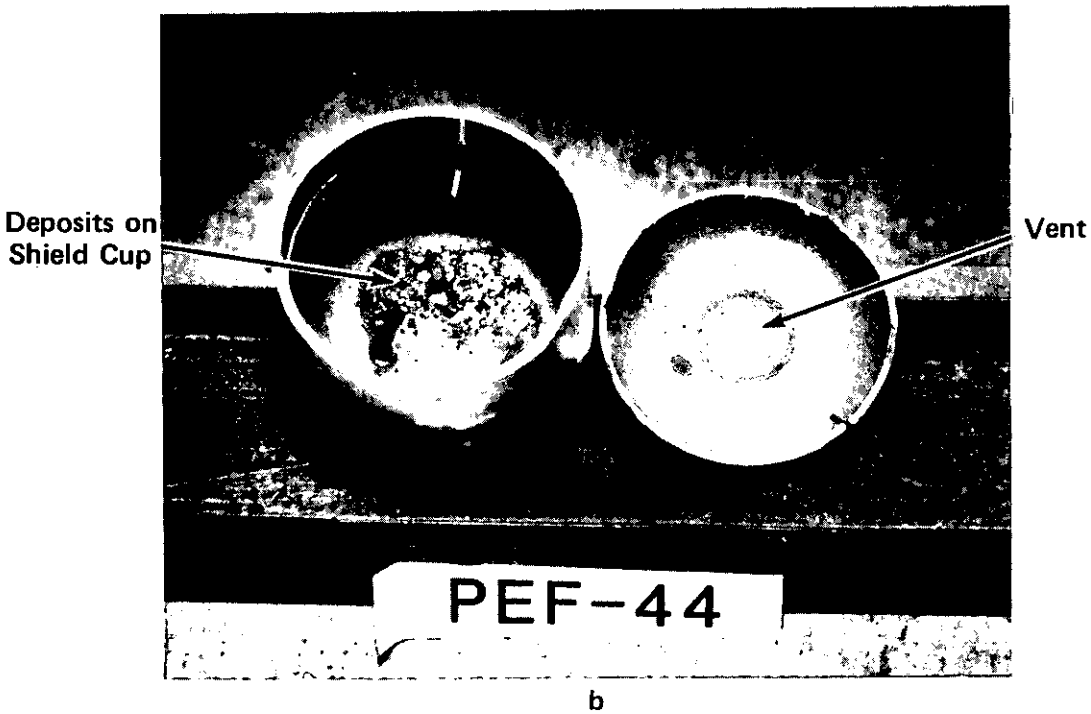

b

FIGURE 10. (a) Surface Deposits Around Vent Hole in Capsule 44; (b) Deposits on Inner Surface of Shield Cup.

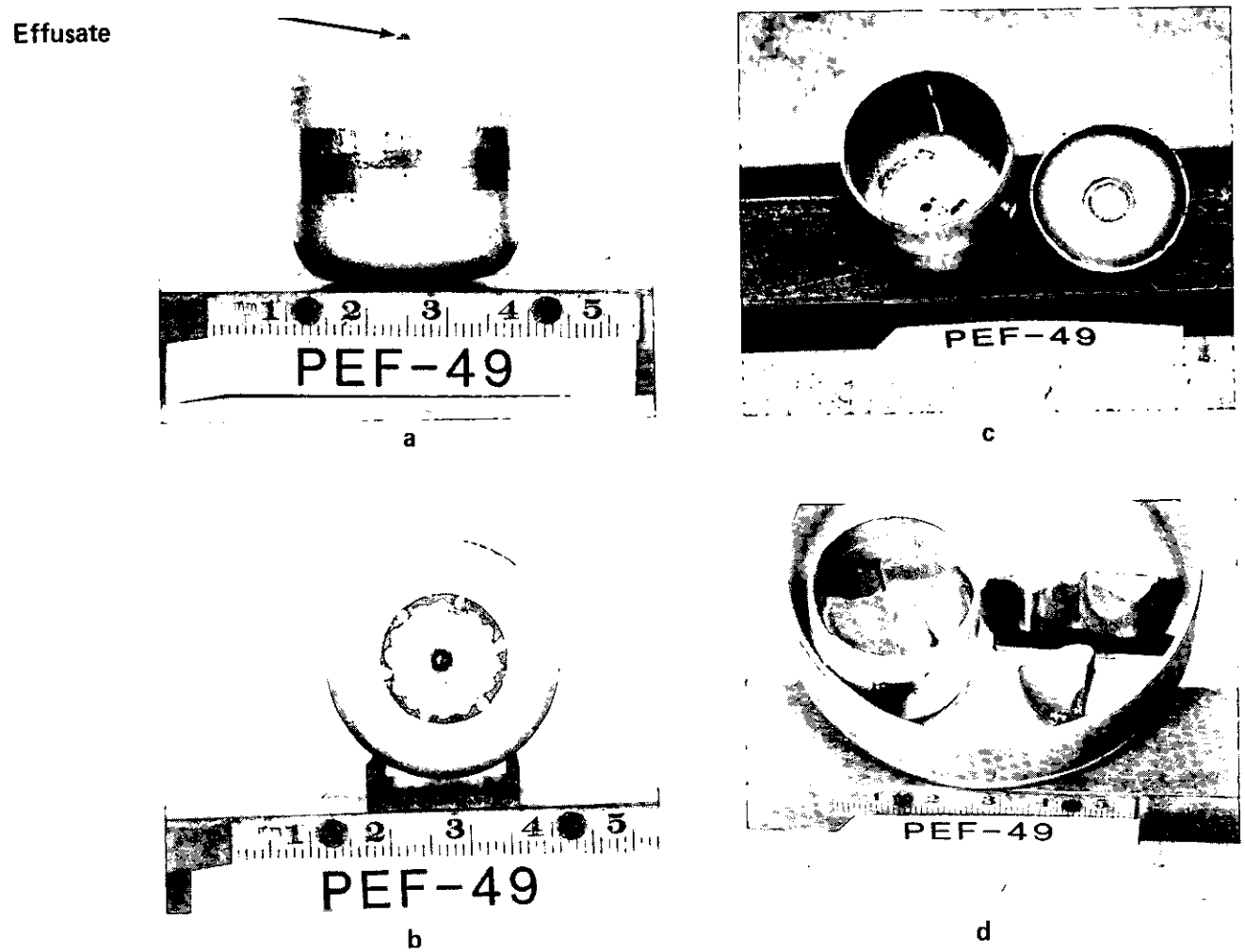

FIGURE 11. (a) Effusate Rising Above Vent Hole in Capsule 49; (b) End-on View of Vent Hole and Effusate; (c) Inner Surface of Cups; (d) Typical Configuration of PuO_2 Fuel in Capsules.

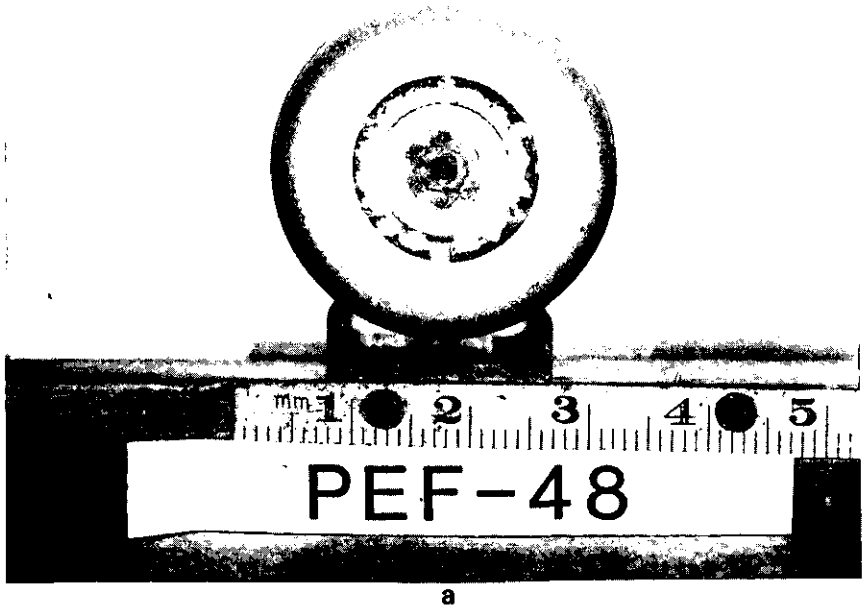

a

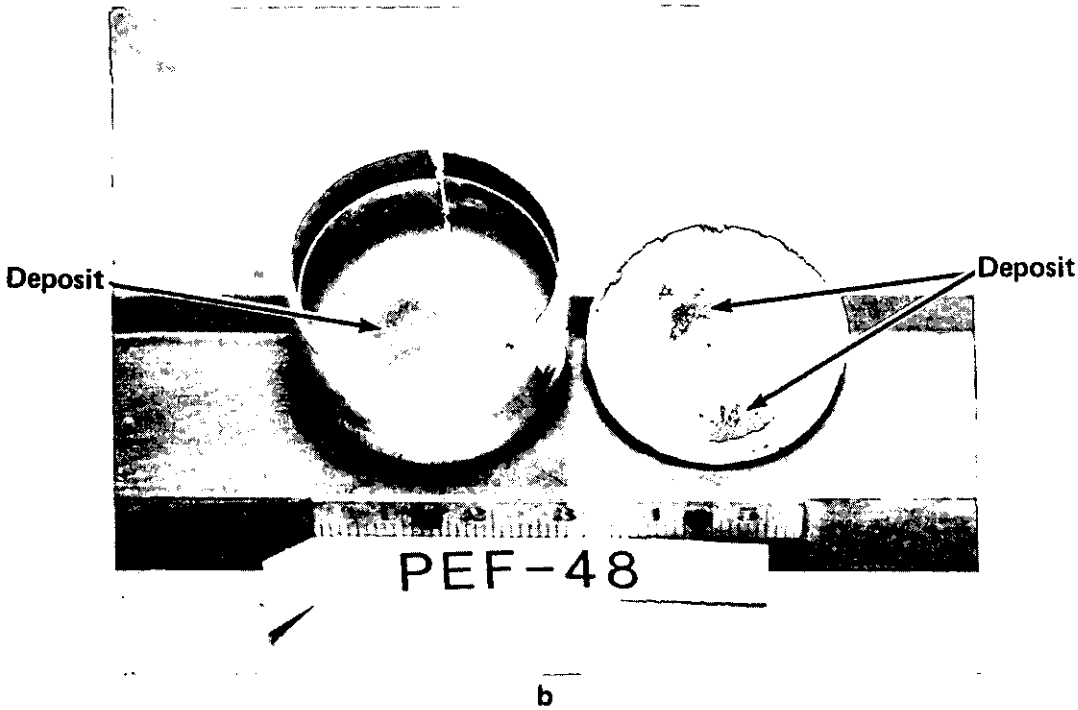

b

FIGURE 12. (a) Surface Deposits Around Vent Hole in Capsule 48; (b) Deposits on Inner Surface of Cups.

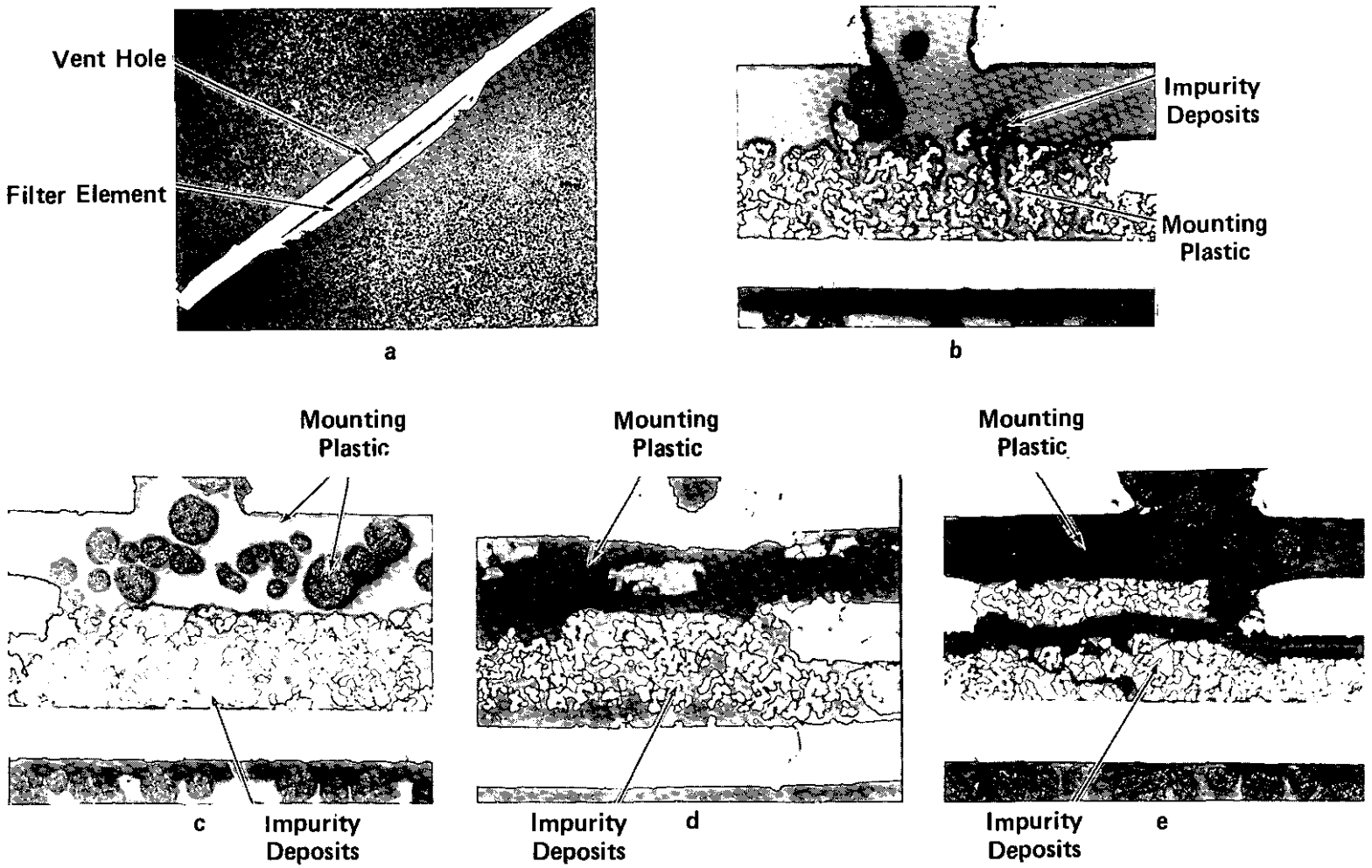

FIGURE 13. Impurity Deposits in Filter Elements (a) Configuration of a Typical GPHS Vent; (b) Vent, Capsule 45; (c) Vent, Capsule 44; (d) Vent, Capsule 48; (e) Vent, Capsule 49.

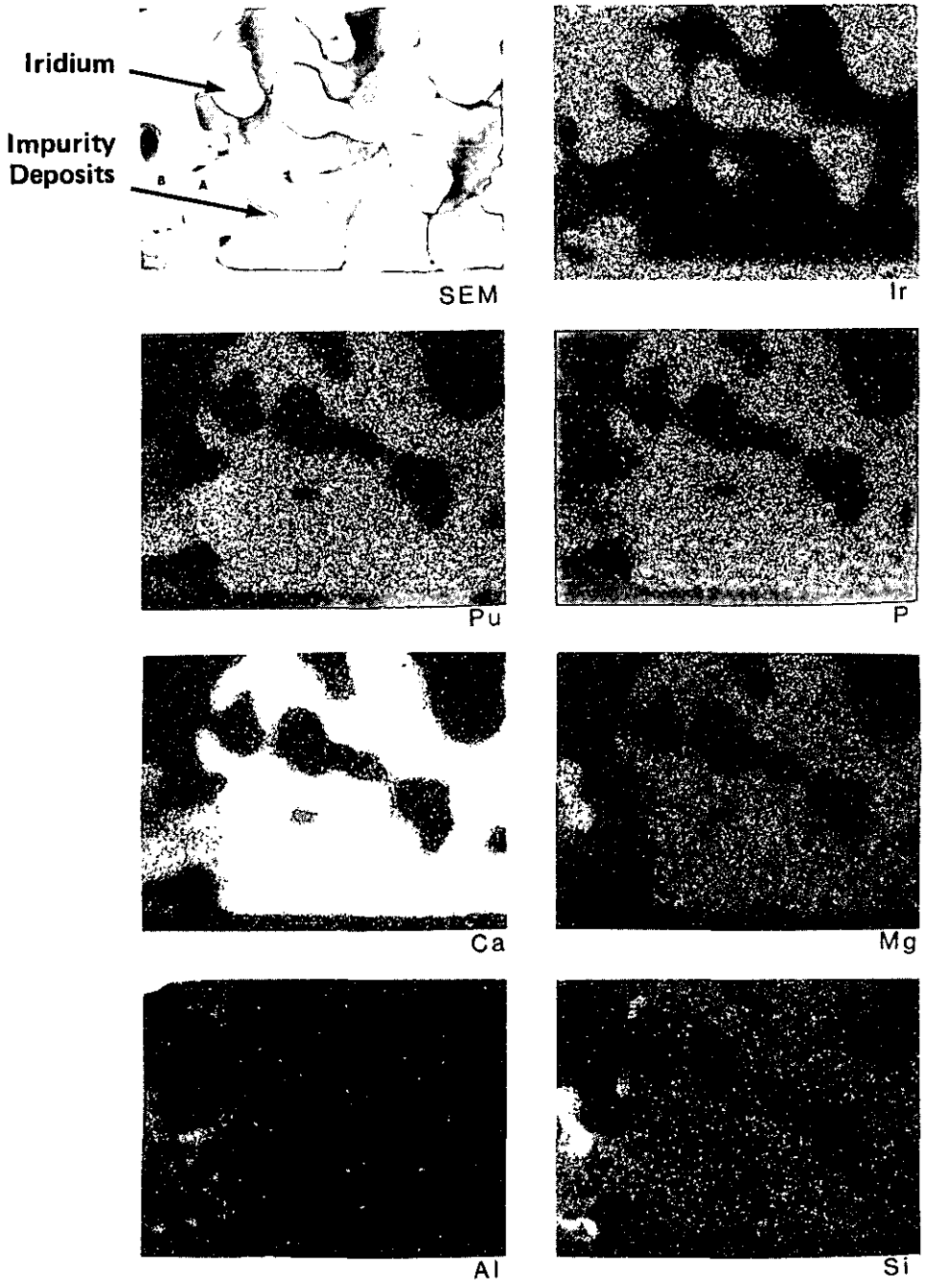

FIGURE 14. Microprobe Electron Dot Images of Impurity Deposits in Filter Element of Capsule 48.

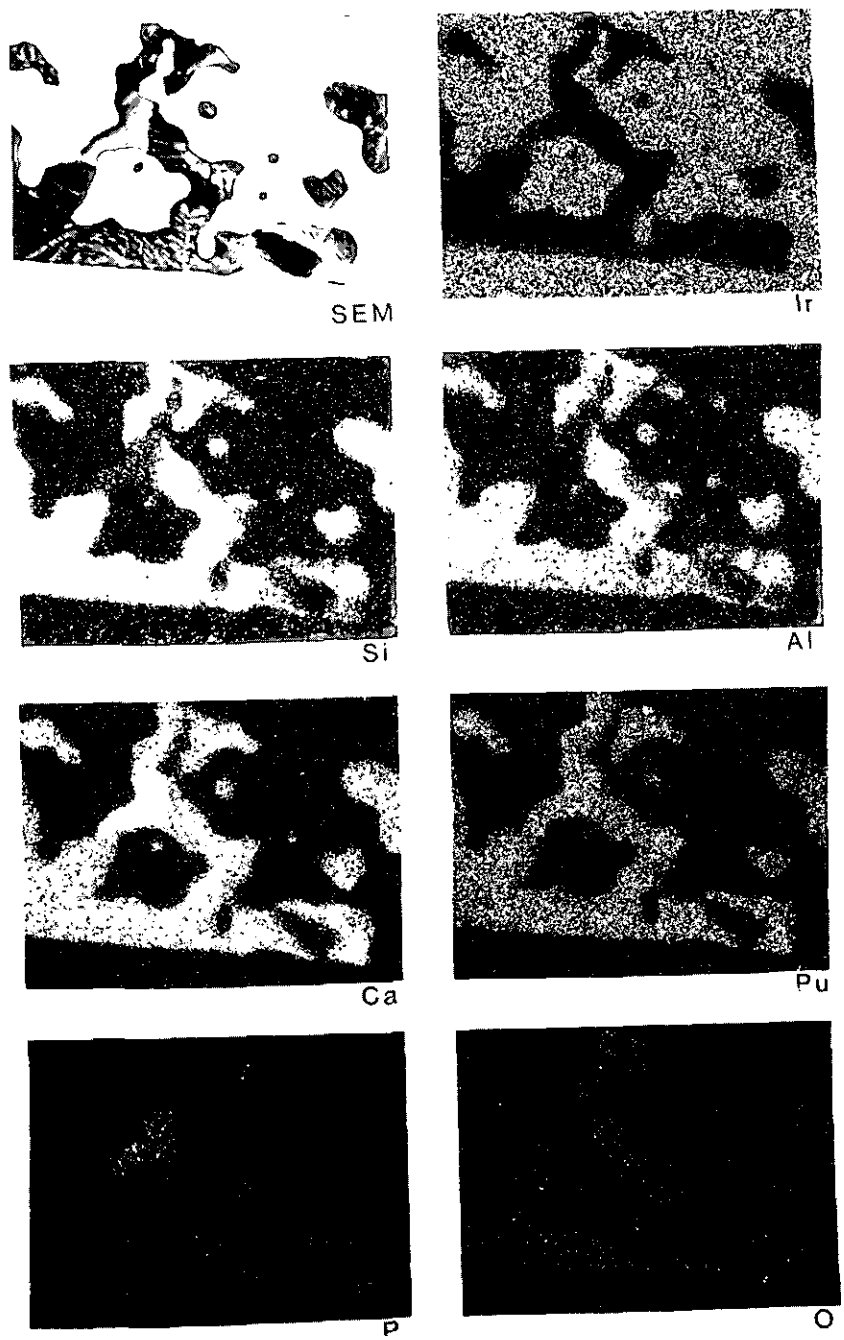

FIGURE 15. Microprobe Electron Dot Images of Impurity Deposits in Filter Element of Capsule 49.

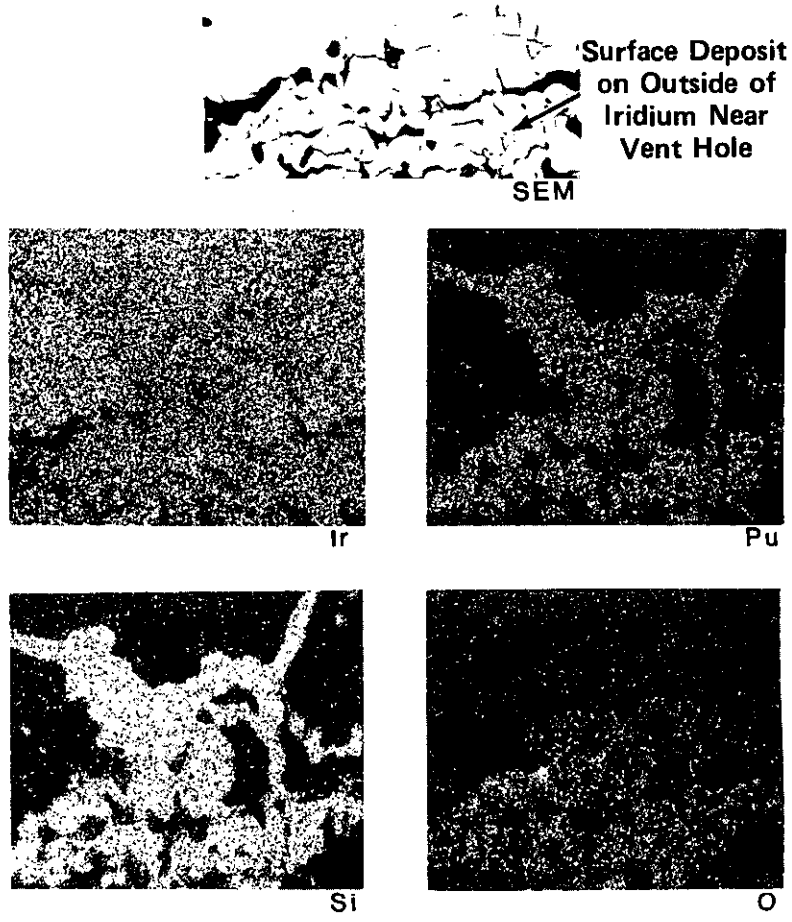

FIGURE 16. Microprobe Electron Dot Images of Ir - Si - Pu Intermetallic Formed at Outside Surface of Capsule 48 Near Vent Hole.

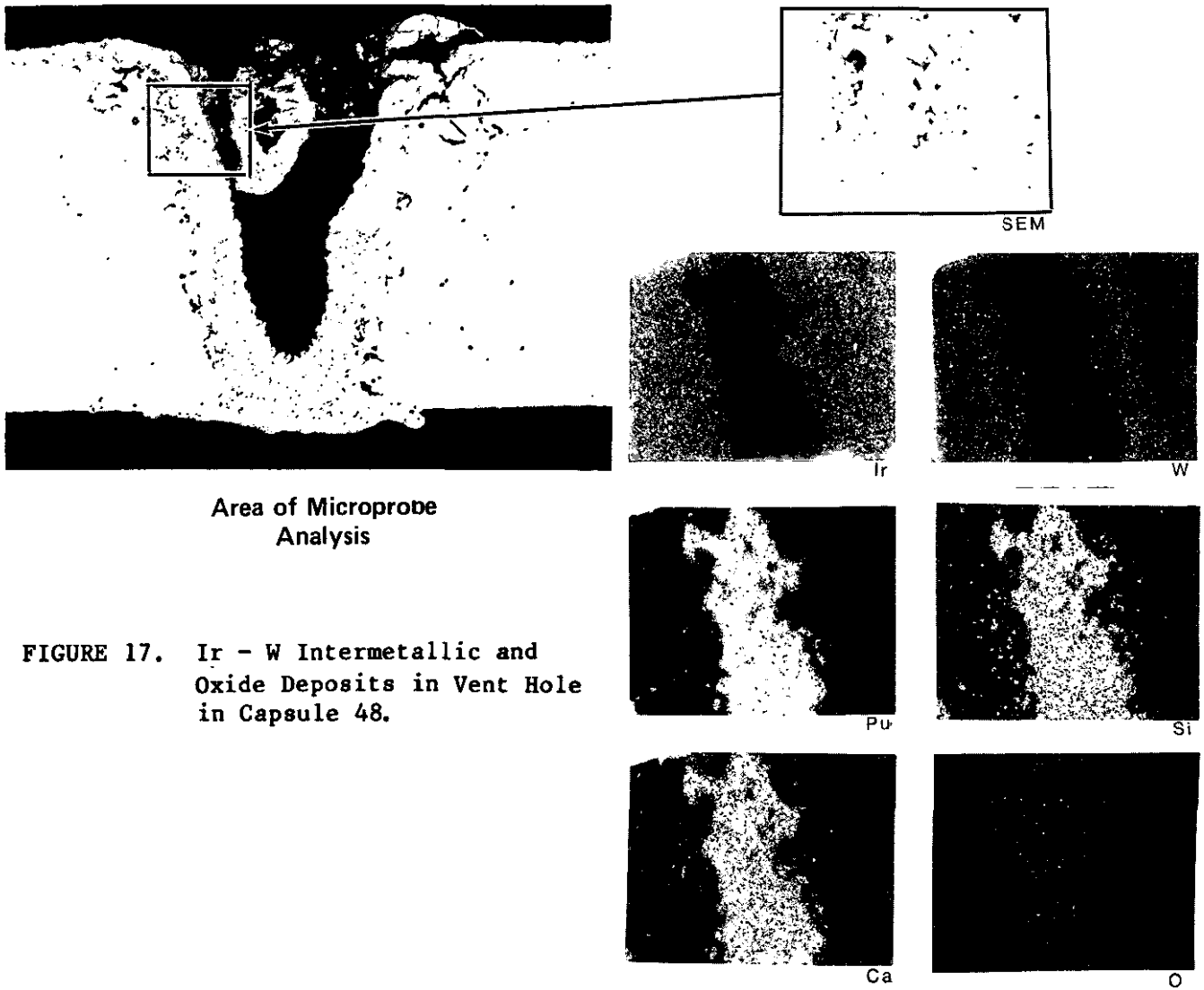

Area of Microprobe Analysis

FIGURE 17. Ir - W Intermetallic and Oxide Deposits in Vent Hole in Capsule 48.

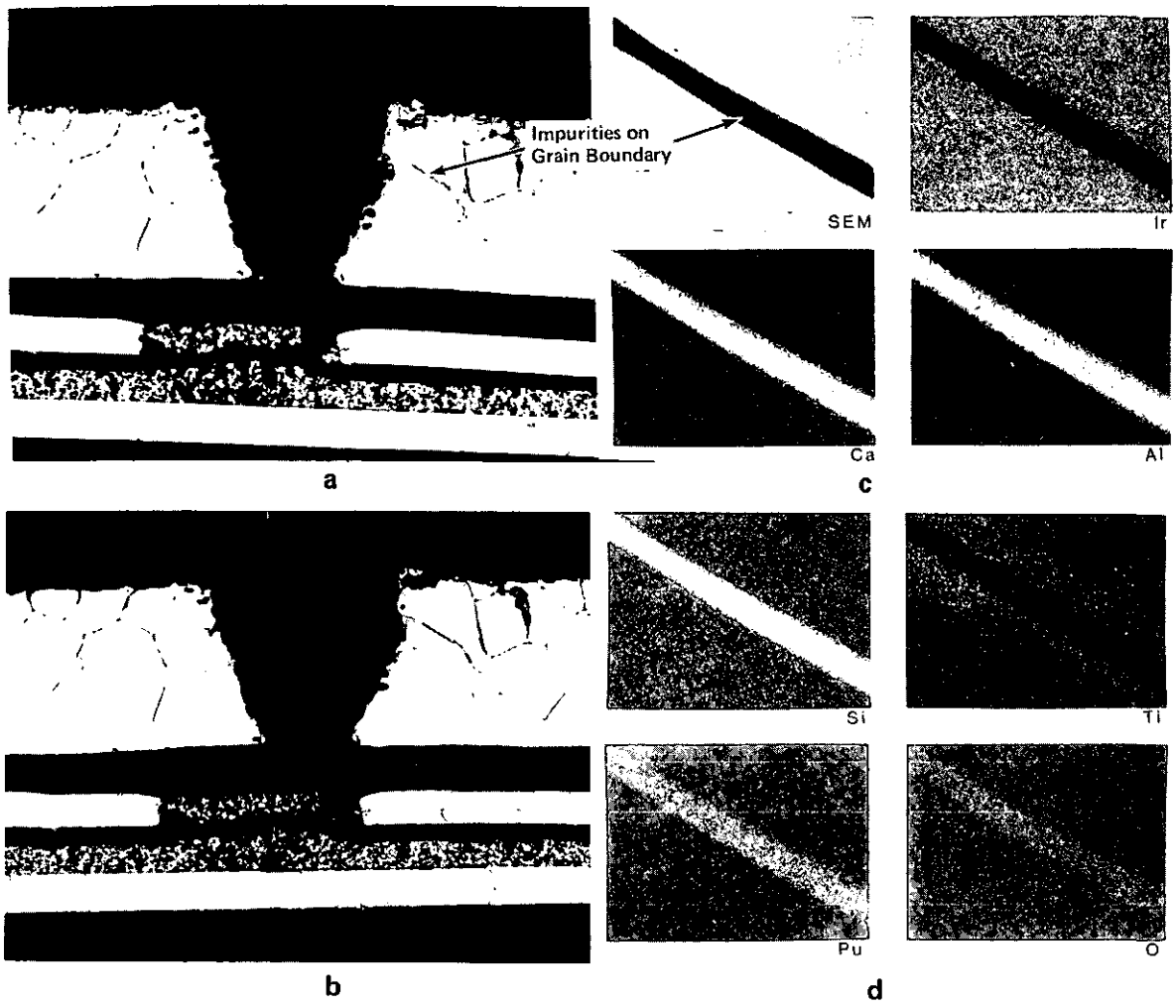

FIGURE 18. Deposits of Ca, Al, and Si in Iridium Grain Boundaries Near Vent Hole of Capsule 49: (a) Impurities Decorating Grain Boundaries in As-Polished Iridium; (b) Etched to Reveal Grain Boundaries; (c)-(d) Microprobe Electron Dot Images of Grain Boundary Deposits in Region Shown in (a).